

New theoretical results for $2\nu\beta\beta$ decay within a fully renormalized proton-neutron random-phase approximation approach with the gauge symmetry restored

C. M. Raduta,¹ A. A. Raduta,^{1,2} and I. I. Ursu¹¹*Department of Theoretical Physics, Horia Hulubei National Institute of Physics and Nuclear Engineering, P.O. Box MG6, Bucharest, Romania*²*Academy of Romanian Scientists, 54 Splaiul Independentei, Bucharest 050094, Romania*

(Received 2 June 2011; revised manuscript received 17 November 2011; published 27 December 2011)

A many-body Hamiltonian involving the mean field for a projected spherical single-particle basis, the pairing interactions for like nucleons, a repulsive dipole-dipole proton-neutron interaction in the particle-hole channel, and an attractive dipole-pairing interaction is treated by a gauge-restored and fully renormalized proton-neutron quasiparticle random-phase approximation formalism. The resulting wave functions and energies for the parent and the daughter nuclei are used to calculate the $2\nu\beta\beta$ decay rate and the process half-life for the emitters: ^{48}Ca , ^{76}Ge , ^{82}Se , ^{96}Zr , ^{104}Ru , ^{110}Pd , $^{128,130}\text{Te}$, $^{148,150}\text{Nd}$, ^{154}Sm , and ^{160}Gd . The results of our calculations are compared with the corresponding experimental data as well as with those obtained through other methods. The Ikeda sum rule is obeyed.

DOI: [10.1103/PhysRevC.84.064322](https://doi.org/10.1103/PhysRevC.84.064322)

PACS number(s): 23.40.Hc, 21.10.Tg, 21.60.Jz

I. INTRODUCTION

The $2\nu\beta\beta$ process is interesting in itself but is also very attractive because it constitutes a test for the nuclear matrix elements (MEs) which are used for the process of $0\nu\beta\beta$ decay. The discovery of this process may provide an answer to the fundamental question of whether the neutrino is a Majorana or a Dirac particle. The development of the subject has been described in several review papers [1–7]. The present paper refers to the $2\nu\beta\beta$ process, which is conceived as consisting of two consecutive and virtual single β^- decays. The formalism yielding closest results to the experimental data is the proton-neutron quasiparticle random-phase approximation ($pnQRPA$) which includes the particle-hole (p-h) and particle-particle (p-p) interactions as independent two-body interactions. The second leg of the $2\nu\beta\beta$ process is very sensitive to changes in the relative strength of the latter interaction, denoted hereafter by g_{pp} . It is worth mentioning that the p-h interaction is repulsive while the p-p one is attractive. Consequently, there is a critical value of g_{pp} for which the first root of the $pnQRPA$ equation vanishes. Actually, this is the signal that the $pnQRPA$ approach is no longer valid. Moreover, the g_{pp} value which corresponds to a transition amplitude that agrees with the corresponding experimental data is close to the mentioned critical value. That means that the result is not stable to the addition of corrections to the RPA picture. An improvement for the $pnQRPA$ was achieved by one of us (A.A.R.), in collaboration, in Refs. [8,9], by using a boson expansion procedure. Another procedure, proposed in Ref. [10], renormalizes the dipole two-quasiparticle operators by replacing the scalar components of their commutators with their average values. Such a renormalization is, however, inconsistently achieved since the scattering operators do not participate in the renormalization process. This lack of consistency was removed in Refs. [11,12] where a fully renormalized $pnQRPA$ (FR $pnQRPA$) is proposed.

Unfortunately, all higher $pnQRPA$ procedures mentioned above have the common drawback of violating the Ikeda

sum rule (ISR) by an amount of about 20–30% [13]. It is believed that this violation is caused by the gauge symmetry breaking. Consequently, a method of restoring this symmetry was formulated by two of us (A.A.R. and C.M.R.) in Ref. [14].

Recently [15,16], the results of Ref. [14] were improved in two respects: (a) aiming at providing a unitary description of the process for situations when the involved nuclei are spherical or deformed, here we use the projected spherical single-particle basis defined in Ref. [17] and used for double- β decay in Refs. [18,19]; (b) the space of proton-neutron dipole configurations is split into three subspaces, one being associated with the single- β^- decay, one with the single- β^+ process, and one spanned by the unphysical states. A set of GRFR $pnQRPA$ equations is written in the first two subspaces mentioned above, by linearizing the equations of motion of the basic transition operators corresponding to the two coupled processes.

In the present paper we apply the equations derived by the GRFR $pnQRPA$ for the $2\nu\beta\beta$ processes $^{48}\text{Ca} \rightarrow ^{48}\text{Ti}$, $^{76}\text{Ge} \rightarrow ^{76}\text{Se}$, $^{82}\text{Se} \rightarrow ^{82}\text{Kr}$, $^{96}\text{Zr} \rightarrow ^{96}\text{Mo}$, $^{104}\text{Ru} \rightarrow ^{104}\text{Pd}$, $^{110}\text{Pd} \rightarrow ^{110}\text{Cd}$, $^{128}\text{Te} \rightarrow ^{128}\text{Xe}$, $^{130}\text{Te} \rightarrow ^{130}\text{Xe}$, $^{148}\text{Nd} \rightarrow ^{148}\text{Sm}$, $^{150}\text{Nd} \rightarrow ^{150}\text{Sm}$, $^{154}\text{Sm} \rightarrow ^{154}\text{Gd}$, and $^{160}\text{Gd} \rightarrow ^{160}\text{Dy}$. New arguments supporting the formalism are given. Moreover, owing to the specific experimental data available, a new procedure for fixing the strengths of the two-body p - n interactions is presented. A detailed comparison to other models aiming at being realistic and at the same time at fulfilling the Ikeda sum rule is mentioned.

The results are described according to the following plan. The model Hamiltonian is given in Sec. II where, also, the FR $pnQRPA$ approach is briefly discussed. The projected gauge of FR $pnQRPA$ (GRFR $pnQRPA$) is the objective of Sec. III. The Gamow-Teller (GT) amplitude for the $2\nu\beta\beta$ process is given in Sec. IV. Numerical applications are shown in Sec. V, while the final conclusions are drawn in Sec. VI.

II. THE MODEL HAMILTONIAN

A. Projected spherical single-particle basis

In Ref. [17], one of us, (A.A.R., in collaboration), introduced an angular-momentum-projected single-particle basis which seems to be appropriate for the description of the single-particle motion in a deformed mean field generated by the particle-core interaction. Aiming at a self-contained presentation, we give here the main ingredients of the method used in that reference. The single-particle mean field is determined by a particle-core Hamiltonian:

$$\tilde{H} = H_{\text{sm}} + H_{\text{core}} - M\omega_0^2 r^2 \sum_{\lambda=0,2} \sum_{-\lambda \leq \mu \leq \lambda} \alpha_{\lambda\mu}^* Y_{\lambda\mu}. \quad (2.1)$$

Here H_{sm} denotes the spherical shell model Hamiltonian while H_{core} is a harmonic quadrupole boson (b_μ^\dagger) Hamiltonian associated with a phenomenological core. The interaction of the two subsystems is accounted for by the third term of Eq. (2.1), written in terms of the shape coordinates α_{00} and $\alpha_{2\mu}$. The monopole shape coordinate can be expressed in terms of the quadrupole coordinates owing to the volume conservation condition. The quadrupole shape coordinates are related to the quadrupole boson operators by the canonical transformation

$$\alpha_{2\mu} = \frac{1}{k\sqrt{2}} [b_{2\mu}^\dagger + (-)^\mu b_{2,-\mu}], \quad (2.2)$$

where k is an arbitrary C number. Averaging \tilde{H} on the eigenstates of H_{sm} , hereafter denoted by $|nljm\rangle$, one obtains a deformed boson Hamiltonian whose ground state is described by the coherent state

$$\Psi_g = \exp[d(b_{20}^\dagger - b_{20})]|0\rangle_b, \quad (2.3)$$

with $|0\rangle_b$ standing for the vacuum state of the boson operators and d a real parameter which simulates the nuclear deformation. Indeed, averaging the quadrupole moment operator

$$Q_{20} = q_0(b_{20}^\dagger + b_{20}), \quad (2.4)$$

with the above mentioned coherent state, one obtains

$$\langle \Psi_g | Q_{20} | \Psi_g \rangle = 2q_0 d. \quad (2.5)$$

The average of \tilde{H} on Ψ_g is similar to the Nilsson Hamiltonian [20]. Because of these properties, it is expected that the best trial functions to be used to generate, through projection, a spherical basis are

$$\Psi_{nlj}^{\text{pc}} = |nljm\rangle \Psi_g. \quad (2.6)$$

The superscript ‘‘pc’’ appearing in the left-hand side of the above equation suggests that the product function is associated with the particle-core system. The projected states are obtained in the usual manner by acting on these deformed states with the projection operator

$$P_{\text{MK}}^I = \frac{2I+1}{8\pi^2} \int D_{\text{MK}}^I(\Omega) \hat{R}(\Omega) d\Omega. \quad (2.7)$$

A certain subset of projected states is orthogonal:

$$\Phi_{\text{nlj}}^{\text{IM}}(d) = \mathcal{N}_{\text{nlj}}^I P_{\text{MI}}^I [|nljI\rangle \Psi_g]. \quad (2.8)$$

The main properties of these projected spherical states are as follows: (i) They are orthogonal with respect to the quantum numbers I and M . (ii) Although the projected states are associated with the particle-core system, they can be used as a single-particle basis. Indeed, when a matrix element of a particlelike operator is calculated, the integration on the core collective coordinates is performed first, which results in obtaining a final factorized expression: one factor carries the dependence on deformation and one is a spherical shell model matrix element. (iii) The connection between the nuclear deformation and the parameter d entering the definition of the coherent state (2.4) is readily obtained by requiring that the strength of the particle-core quadrupole-quadrupole interaction be identical to the Nilsson deformed term of the mean field:

$$\frac{d}{k} = \sqrt{\frac{2\pi}{45}} (\Omega_\perp^2 - \Omega_z^2). \quad (2.9)$$

Here Ω_\perp and Ω_z denote the frequencies of Nilsson’s mean field, related to the deformation $\delta = \sqrt{45/16\pi} \beta$ by

$$\Omega_\perp = \left(\frac{2+\delta}{2-\delta} \right)^{1/3}, \quad \Omega_z = \left(\frac{2+\delta}{2-\delta} \right)^{-2/3}. \quad (2.10)$$

The average of the particle-core Hamiltonian $H' = \tilde{H} - H_{\text{core}}$ on the projected spherical states defined by (2.8) approximates quite well the single-particle energies associated with the eigenstates of the deformed single-particle mean field:

$$\epsilon_{\text{nlj}}^I = \langle \Phi_{\text{nlj}}^{\text{IM}}(d) | H' | \Phi_{\text{nlj}}^{\text{IM}}(d) \rangle. \quad (2.11)$$

These matrix elements were analytically expressed in Ref. [17]. Since the core contribution does not depend on the quantum numbers of the single-particle energy level, it produces a shift for all energies and therefore is omitted in Eq. (2.11). However, when the ground-state energy variation against deformation is studied, this term should be considered as well.

Note that the average values ϵ_{nlj}^I may be viewed as approximate expressions for the single-particle energies in deformed Nilsson orbits. We may account for the deviations from the exact eigenvalues by considering, later on, the off-diagonal matrix elements of the particle-core interaction when a specific treatment of the many-body system is applied.

The parameters involved in H_{sm} were taken from Ref. [21]. The deformation parameter was fixed by fitting the strength of the $E2$ transition to the first collective 2^+ . The canonicity parameter can be determined by requiring that the energy spacings between two particular adjacent single-particle energy levels in the Nilsson and present formalism are the same. Because of these features the dependence of the new single-particle energies on the deformation parameter d is similar to that shown by the Nilsson model for the single-particle energies [20] as a function of the quadrupole nuclear deformation, β . For illustration the dependence on d of the proton single-particle energies is shown in Fig. 1 for ^{154}Sm .

Although the energy levels are similar to those of the Nilsson model, the quantum numbers in the two schemes are different. Indeed here we generate from each j a multiplet of $(2j+1)$ states as I , which plays the role of the Nilsson quantum number Ω , runs from $1/2$ to j , and moreover the energies corresponding to the quantum numbers K and $-K$ are equal to each other.

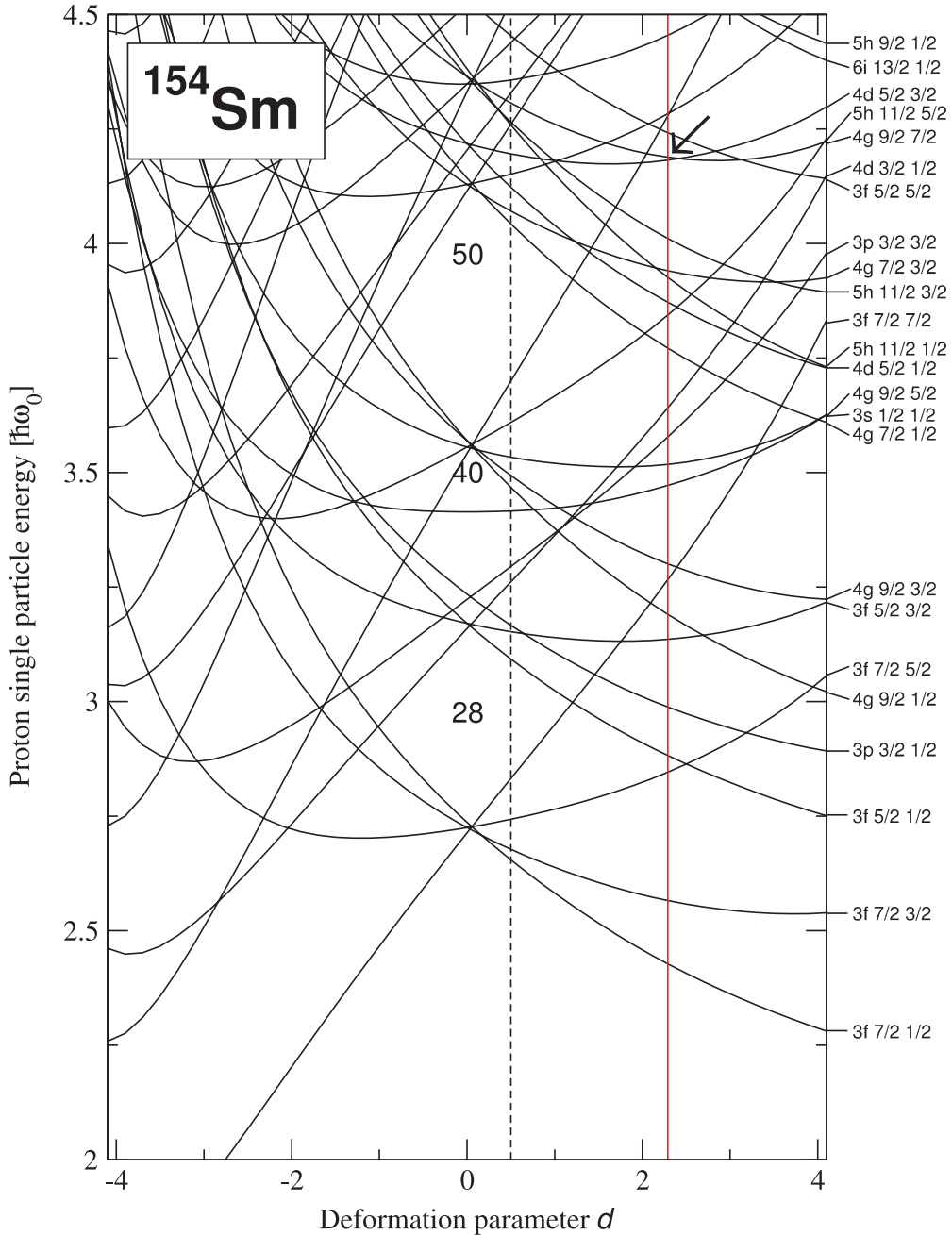


FIG. 1. (Color online) Proton single-particle energies for ^{154}Sm . Vertical full line corresponds to the deformation parameter d used in the present calculations, while the dashed vertical line corresponds to that deformation which minimizes the proton system energy. The difference between the two values may be washed out if the contribution of H_{core} to the total energy to be minimized is taken into account. The Fermi level is indicated by an arrow.

On the other hand, for a given l there are $2l + 1$ degenerate substates while the Nilsson states are only doubly degenerate. As explained in Ref. [17], the redundancy problem can be solved by changing the normalization of the model functions:

$$\langle \Phi_{\alpha}^{\text{IM}} | \Phi_{\alpha}^{\text{IM}} \rangle = 1 \implies \sum_M \langle \Phi_{\alpha}^{\text{IM}} | \Phi_{\alpha}^{\text{IM}} \rangle = 2. \quad (2.12)$$

Because of this weighting factor the particle density function provides the consistent result that the number of particles which can be distributed on the $(2l + 1)$ substates is at most

2, which agrees with the Nilsson model. Here α stands for the set of shell model quantum numbers nlj . Owing to this normalization, the states $\Phi_{\alpha\text{IM}}$ used to calculate the matrix elements of a given operator should be multiplied by the weighting factor $\sqrt{2/(2l + 1)}$. The role of the core component is to induce a quadrupole deformation for the matrix elements of the operators acting on the particle degrees of freedom. For any such an operator the following factorization holds:

$$\langle \Phi_{nlj}^I | |T_k| | \Phi_{n'l'j'}^{I'} \rangle = f_{nlj}^{n'l'j'I'} \langle nlj || T_k || n'l'j' \rangle. \quad (2.13)$$

The factor f carries the dependence on the deformation parameter d , while the other factor is just the reduced matrix element corresponding to the spherical shell model states.

In conclusion, the projected single-particle basis is defined by Eq. (2.8). Although these states are associated with a particle-core system, they can be used as a single-particle basis because of the properties mentioned above. Therefore the projected states might be thought of as eigenstates of an effective rotationally invariant fermionic one-body Hamiltonian H_{eff} , with the corresponding energies given by Eq. (2.11):

$$H_{\text{eff}}\Phi_{\alpha}^{\text{IM}} = \epsilon_{\alpha}^I(d)\Phi_{\alpha}^{\text{IM}}. \quad (2.14)$$

This definition should be supplemented by the request that the matrix elements of any operator between states $\Phi_{\alpha}^{\text{IM}}$ and $\Phi_{\alpha'}^{I'M'}$ are given by Eq. (2.13). Because of these features, these states can be used as a single-particle basis to treat many-body Hamiltonians that involve one-body operators. This is the case of Hamiltonians with two-body separable forces. As a matter of fact, this type of Hamiltonian is used in the present paper.

In the vibrational limit $d \rightarrow 0$, the projected spherical basis goes to the spherical shell model basis and ϵ_{nlj}^I to the eigenvalues of H_{sm} .

For the sake of completeness, we paid attention also to the general two-body interaction. In this way one hopefully avoids a possible erroneous interpretation of the product of two projected single-particle states. Thus in Ref. [13] we proved that the matrix elements of a two-body interaction corresponding to the present scheme are very close to the matrix elements corresponding to spherical states projected from a deformed product state with one factor as a product of two spherical single-particle states, and a second factor consisting of a common collective core wave function. The small discrepancies of the two types of matrix elements could be washed out by using slightly different strengths for the two-body interaction in the two methods. Because of this property the basis (2.8) might be used for studying any two-body interaction.

B. Fully renormalized pn QRPA treatment

In the present work we wish to describe unitarily the Gamow-Teller two-neutrino double- β decay of even-even nuclei with and without spherical symmetry. In our treatment the Fermi transitions, contributing about 20%, and the ‘‘forbidden’’ transitions are ignored, which is a reasonable approximation for the two-neutrino double- β decay in medium and heavy nuclei.

We suppose that the states describing the nuclei involved in a $2\nu\beta\beta$ process are described by a many-body Hamiltonian that may be written in the projected spherical basis as

$$H = \sum_{\tau,\alpha,I,M} \frac{2}{2I+1} (\epsilon_{\tau\alpha I} - \lambda_{\tau\alpha}) c_{\tau\alpha\text{IM}}^{\dagger} c_{\tau\alpha\text{IM}} - \sum_{\tau,\alpha,I,I'} \frac{G_{\tau}}{4} P_{\tau\alpha I}^{\dagger} P_{\tau\alpha I'} + 2\chi \sum_{pn;p'n';\mu} \beta_{\mu}^{-}(pn) \beta_{-\mu}^{+}(p'n') (-)^{\mu} - 2\chi_1 \sum_{pn;p'n';\mu} P_{\mu}^{-}(pn) P_{-\mu}^{+}(p'n') (-)^{\mu}, \quad (2.15)$$

where $c_{\tau\alpha\text{IM}}^{\dagger}$ ($c_{\tau\alpha\text{IM}}$) denotes the creation (annihilation) operator of one nucleon of the type $\tau (=p, n)$ in the state $\Phi_{\alpha}^{\text{IM}}$, with α being an abbreviation for the set of quantum numbers nlj . The Hamiltonian H contains the mean-field term, the pairing interactions for alike nucleons whose strengths are denoted by G_{τ} , and the Gamow-Teller dipole-dipole interaction in the p-h and p-p channels, characterized by the strengths χ and χ_1 , respectively.

In order to simplify the notation, hereafter the set of quantum numbers $\alpha (=nlj)$ will be omitted. Note that the two-body interactions are separable, with the factors defined by the following expressions:

$$P_{\tau I}^{\dagger} = \sum_M \frac{2}{2I+1} c_{\tau\text{IM}}^{\dagger} c_{\tau\text{IM}}^{\dagger},$$

$$\beta_{\mu}^{-}(pn) = \sum_{M,M'} \frac{\sqrt{2}}{\hat{I}} \langle p\text{IM} | \sigma_{\mu} | nI'M' \rangle \frac{\sqrt{2}}{\hat{I}'} c_{p\text{IM}}^{\dagger} c_{nI'M'}, \quad (2.16)$$

$$P_{1\mu}^{-}(pn) = \sum_{M,M'} \frac{\sqrt{2}}{\hat{I}} \langle p\text{IM} | \sigma_{\mu} | nI'M' \rangle \frac{\sqrt{2}}{\hat{I}'} c_{p\text{IM}}^{\dagger} c_{nI'M'}^{\dagger}.$$

The other operators from Eq. (2.15) can be obtained from the above expressions, by Hermitian conjugation.

In the quasiparticle representation, defined by the Bogoliubov-Valatin transformation

$$a_{\tau\text{IM}}^{\dagger} = U_{\tau I} c_{\tau\text{IM}}^{\dagger} - s_{\text{IM}} V_{\tau I} c_{\tau I-M}, \quad s_{\text{IM}} = (-)^{I-M}, \quad (2.17)$$

$$\tau = p, n, \quad U_{\tau I}^2 + V_{\tau I}^2 = 1,$$

the first two terms of H are replaced by the independent quasiparticle (qp) term $\sum E_{\tau I} a_{\tau\text{IM}}^{\dagger} a_{\tau\text{IM}}$, while the p-h and p-p interactions are expressed in terms of the two-qp and the qp dipole density operators:

$$A_{1\mu}^{\dagger}(pn) = \sum C_{m_p m_n}^{I_p I_n} a_{pI_p m_p}^{\dagger} a_{nI_n m_n}^{\dagger},$$

$$A_{1\mu}(pn) = (A_{1\mu}^{\dagger}(pn))^{\dagger}, \quad (2.18)$$

$$B_{1\mu}^{\dagger}(pn) = \sum C_{m_p -m_n}^{I_p I_n} a_{pI_p m_p}^{\dagger} a_{nI_n m_n} (-)^{I_n - m_n},$$

$$B_{1\mu}(pn) = (B_{1\mu}^{\dagger}(pn))^{\dagger}.$$

As shown in Ref. [11], all these operators can be renormalized by making use of the commutation equations

$$[A_{1\mu}(k), A_{1\mu'}^{\dagger}(k')] \approx \delta_{k,k'} \delta_{\mu,\mu'} \left[1 - \frac{\hat{N}_n}{\hat{I}_n^2} - \frac{\hat{N}_p}{\hat{I}_p^2} \right],$$

$$[B_{1\mu}^{\dagger}(k), A_{1\mu'}^{\dagger}(k')] \approx [B_{1\mu}^{\dagger}(k), A_{1\mu'}(k')] \approx 0, \quad (2.19)$$

$$[B_{1\mu}(k), B_{1\mu'}^{\dagger}(k')] \approx \delta_{k,k'} \delta_{\mu,\mu'} \left[\frac{\hat{N}_n}{\hat{I}_n^2} - \frac{\hat{N}_p}{\hat{I}_p^2} \right], \quad k = (I_p, I_n),$$

with \hat{N}_{τ} denoting the quasiparticle number operator of type τ ($=p, n$). Indeed, denoting by $C_{I_p, I_n}^{(1)}$ and $C_{I_p, I_n}^{(2)}$ the averages of the right-hand sides of (2.19) with the renormalized pn QRPA

vacuum state, the renormalized operators defined as

$$\bar{A}_{1\mu}(k) = \frac{1}{\sqrt{C_k^{(1)}}} A_{1\mu}, \quad \bar{B}_{1\mu}(k) = \frac{1}{\sqrt{|C_k^{(2)}|}} B_{1\mu} \quad (2.20)$$

obey the bosonlike commutation relations

$$\begin{aligned} [\bar{A}_{1\mu}(k), \bar{A}_{1\mu'}^\dagger(k')] &= \delta_{k,k'} \delta_{\mu,\mu'}, \\ [\bar{B}_{1\mu}(k), \bar{B}_{1\mu'}^\dagger(k')] &= \delta_{k,k'} \delta_{\mu,\mu'} f_k, \quad f_k = \text{sgn}(C_k^{(2)}). \end{aligned} \quad (2.21)$$

Further, these operators are used to define the phonon operator:

$$\begin{aligned} C_{1\mu}^\dagger &= \sum_k [X(k) \bar{A}_{1\mu}^\dagger(k) + Z(k) \bar{D}_{1\mu}^\dagger(k) - Y(k) \bar{A}_{1-\mu}(k) (-)^{1-\mu} \\ &\quad - W(k) \bar{D}_{1-\mu}(k) (-)^{1-\mu}], \end{aligned} \quad (2.22)$$

where $\bar{D}_{1\mu}^\dagger(k)$ is equal to $\bar{B}_{1\mu'}^\dagger(k')$ or $\bar{B}_{1\mu}(k)$ depending on whether f_k is + or -. The phonon amplitudes are determined by the equations

$$[H, C_{1\mu}^\dagger] = \omega C_{1\mu}^\dagger, \quad [C_{1\mu}, C_{1\mu'}^\dagger] = \delta_{\mu\mu'}. \quad (2.23)$$

Interesting properties for these equations and their solutions were discussed in our previous publications [11,12]. The

formalism defined above was named the fully renormalized proton-neutron quasiparticle random-phase approximation (FrpnQRPA).

III. GAUGE PROJECTION OF THE FULLY RENORMALIZED pnQRPA

The ground state of an (N, Z) nucleus can be excited by the phonon operator, defined above, to a state which is a superposition of components describing the neighboring nuclei $(N-1, Z+1)$, $(N+1, Z-1)$, $(N+1, Z+1)$, $(N-1, Z-1)$. The first two components conserve the total number of nucleons $(N+Z)$ but violate the third component of isospin, T_3 . By contrast, the last two components violate the total number of nucleons but preserve T_3 . Actually, the last two components are those that contribute to the ISR violation. However, one can construct linear combinations of the basic operators $A^\dagger, A, B^\dagger, B$ which excite the nucleus (N, Z) to the nuclei $(N-1, Z+1)$, $(N+1, Z-1)$, $(N+1, Z+1)$, $(N-1, Z-1)$, respectively. These operators are

$$\begin{aligned} \mathcal{A}_{1\mu}^\dagger(pn) &= U_p V_n A_{1\mu}^\dagger(pn) + U_n V_p A_{1,-\mu}(pn) (-)^{1-\mu} + U_p U_n B_{1\mu}^\dagger(pn) - V_p V_n B_{1,-\mu}(pn) (-)^{1-\mu}, \\ \mathcal{A}_{1\mu}(pn) &= U_p V_n A_{1\mu}(pn) + U_n V_p A_{1,-\mu}^\dagger(pn) (-)^{1-\mu} + U_p U_n B_{1\mu}(pn) - V_p V_n B_{1,-\mu}^\dagger(pn) (-)^{1-\mu}, \\ \mathbf{A}_{1\mu}^\dagger(pn) &= U_p U_n A_{1\mu}^\dagger(pn) - V_p V_n A_{1,-\mu}(pn) (-)^{1-\mu} - U_p V_n B_{1\mu}^\dagger(pn) - V_p U_n B_{1,-\mu}(pn) (-)^{1-\mu}, \\ \mathbf{A}_{1\mu}(pn) &= U_p U_n A_{1\mu}(pn) - V_p V_n A_{1,-\mu}^\dagger(pn) (-)^{1-\mu} - U_p V_n B_{1\mu}(pn) - V_p U_n B_{1,-\mu}^\dagger(pn) (-)^{1-\mu}. \end{aligned}$$

In the particle representation these operators have the expressions

$$\begin{aligned} \mathcal{A}_{1\mu}^\dagger(pn) &= -[c_p^\dagger c_n^\dagger]_{1\mu}, \quad \mathcal{A}_{1\mu}(pn) = -[c_p^\dagger c_n^\dagger]_{1\mu}^\dagger, \\ \mathbf{A}_{1\mu}^\dagger(pn) &= [c_p^\dagger c_n^\dagger]_{1\mu}, \quad \mathbf{A}_{1\mu}(pn) = [c_p^\dagger c_n^\dagger]_{1\mu}^\dagger. \end{aligned} \quad (3.1)$$

Thus, the operators from the first row excite the nucleus (N, Z) to the nuclei $(N-1, Z+1)$ and $(N+1, Z-1)$, respectively, while the operators $\mathbf{A}_{1\mu}^\dagger(pn)$ and $\mathbf{A}_{1\mu}(pn)$ bring (N, Z) to $(N+1, Z+1)$ and $(N-1, Z-1)$, respectively. In terms of the new operators, the many-body Hamiltonian is

$$\begin{aligned} H &= \sum_{\tau jm} E_{\tau j} a_{\tau jm}^\dagger a_{\tau jm} + 2\chi \sum_{pn, p'n'; \mu} \sigma_{pn; p'n'} \mathcal{A}_{1\mu}^\dagger(pn) \mathcal{A}_{1\mu}(p'n') \\ &\quad - 2\chi_1 \sum_{pn, p'n'; \mu} \sigma_{pn; p'n'} \mathbf{A}_{1\mu}^\dagger(pn) \mathbf{A}_{1\mu}(p'n'), \quad \sigma_{pn; p'n'} \\ &= \frac{2}{3\hat{I}_n \hat{I}_{n'}} \langle I_p || \sigma || I_n \rangle \langle I_{p'} || \sigma || I_{n'} \rangle, \end{aligned} \quad (3.2)$$

where $E_{\tau l}$ denotes the quasiparticle energy.

At this stage we have to explain why the p-p interaction is not effective, i.e., does not contribute at all within

our approach. Indeed, within the gauge-preserved picture the operators $\mathcal{A}_{1\mu}$ and $\mathbf{A}_{1\mu}^\dagger$ commute with each other. Consequently, the gauge-projected phonon operator cannot comprise terms like $\mathbf{A}_{1\mu}^\dagger$ since they violate the total number of nucleons. If the mentioned commutator were different from zero, but equal to the average with the new vacuum state of its scalar part, then the equations of motion for the operators $\mathcal{A}_{1\mu}$ and $\mathcal{A}_{1\mu}^\dagger$ would be linear not only in the nucleon-number-conserving operators, but also in those which do not conserve the total number operator. In order that the equations of motion constitute a closed algebra, we have to add the equations corresponding to the number-nonconserving operators. Consequently, the phonon operator is a linear combination of both nucleon-number-conserving and -nonconserving terms. It is clear now that in order to conserve the nucleon total number it is necessary to accept that the operators $\mathcal{A}_{1\mu}$ and $\mathbf{A}_{1\mu}^\dagger$ commute with each other. In this context the p-p interaction becomes inefficient for properties described by gauge-preserving wave functions and therefore we have to ignore it. In this respect our formalism contrasts with the picture of Ref. [22] where the phonon operator commutes with the nucleon total number operator and at the same time the p-p interaction contributes to the renormalized pnQRPA equations.

However, in aiming at a quantitative description of the double- β process, the presence of an attractive proton-neutron interaction is necessary. For this reason we replace the p - p interaction, which is ineffective anyway, with a dipole-pairing interaction:

$$\Delta H = -X_{dp} \sum_{\substack{pn:p' \\ n':\mu}} (\beta_{\mu}^{-}(pn)\beta_{-\mu}^{-}(p'n') + \beta_{-\mu}^{+}(p'n')\beta_{\mu}^{+}(pn)) \times (-1)^{1-\mu}. \quad (3.3)$$

We remark that the two terms of ΔH change the charge by $+2$ and -2 units, respectively, and therefore one may think that it is not justified within the meson-dynamic theory of nuclear forces. That is not true, if we keep in mind the isospin charge independence property of the nuclear forces. Also, we note that ΔH is Hermitian and invariant to rotation. This Hamiltonian should be looked at as an effective Hamiltonian in the same manner as is the standard pairing Hamiltonian. Indeed, within the BCS approximation the initial pairing Hamiltonian is replaced by an effective one $\Delta(c^{\dagger}c^{\dagger})_0 + \Delta^{*}(cc)_0$, with c^{\dagger} (c) denoting the single-particle creation (annihilation) operator. This Hamiltonian also does not preserve the charge, but this is consistent with the trial variational state $|\text{BCS}\rangle$, which is a mixture of components with different even numbers of particles. In the present case the pn QRPA state is built on top of the BCS ground state, which is a product of the BCS states for protons and neutrons, respectively, so that a linear superposition of components with different isospin third components T_3 is obtained. Of course, at the BCS level T_3 is preserved on average. Therefore, in the quasiparticle picture the condition that the Hamiltonian commutes separately with the proton and neutron number operators is anyway not satisfied by any of the terms composing the model Hamiltonian. Note that ΔH commutes with the total number of nucleons and preserves this feature after the linearization procedure is performed, contributing to the equations of motion of the basic operators with the gauge restored. Concerning the T_3 symmetry, let us denote by \mathcal{N}_{τ} the τ ($=p, n$) particle number operators, respectively, and calculate the commutator

$$[\Delta H, \mathcal{N}_p - \mathcal{N}_n] = 4X_{dp} \sum_{\substack{pn:p' \\ n':\mu}} (\beta_{\mu}^{-}(pn)\beta_{-\mu}^{-}(p'n') - \beta_{-\mu}^{+}(p'n')\beta_{\mu}^{+}(pn))(-1)^{1-\mu}. \quad (3.4)$$

Note that the right-hand side of the above equation is an anti-Hermitian operator. Consequently, its average value with any state is vanishing. In particular it vanishes if the chosen state is the BCS ground state or the vacuum state of the GPFR pn QRPA phonon operator. In conclusion, in the present formalism the third isospin component is conserved on average. Clearly this happens since while one term of ΔH increases the charge by two units the other term decreases it by the same amount. Note that this isospin-nonconserving term shows up even at the level of the standard pn QRPA. Indeed within this formalism the two-body interaction is

approximated by a linear combination of the operators

$$A_{1\mu}^{\dagger}(pn)A_{1\mu}(pn), (-1)^{1-\mu}(A_{1\mu}^{\dagger}(pn)A_{1-\mu}^{\dagger}(pn) + A_{1,-\mu}(pn)A_{1\mu}(pn)). \quad (3.5)$$

Writing these terms in the particle representation, one finds that the effective two-body interaction comprises, among other terms, a term that is proportional to ΔH . Therefore, in a formalism using an approximation that violates the T_3 symmetry, the use of a Hamiltonian ΔH which does not preserve the T_3 component does not produce a special inconsistency.

Writing the model Hamiltonian in the quasiparticle representation, one obtains

$$H = \sum_{\tau jm} E_{\tau j} a_{\tau jm}^{\dagger} a_{\tau jm} + 2\chi \sum_{pn, p'n'; \mu} \sigma_{pn, p'n'} A_{1\mu}^{\dagger}(pn) A_{1\mu}(p'n') - X_{dp} \sum_{\substack{pn:p' \\ n':\mu}} \sigma_{pn, p'n'} (A_{1\mu}^{\dagger}(pn) A_{1,-\mu}^{\dagger}(p'n') + A_{1,-\mu}(p'n') A_{1\mu}(pn)) (-1)^{1-\mu}. \quad (3.6)$$

The equations of motion of the operators defining the phonon operator are determined by the commutation relations

$$[A_{1\mu}(pn), A_{1\mu'}^{\dagger}(p'n')] \approx \delta_{\mu, \mu'} \delta_{j_p, j_{p'}} \delta_{j_n, j_{n'}} \times \left[U_p^2 - U_n^2 + \frac{U_n^2 - V_n^2}{\hat{I}_n^2} \hat{N}_n - \frac{U_p^2 - V_p^2}{\hat{I}_p^2} \hat{N}_p \right]. \quad (3.7)$$

The quasiboson approximation replaces the right-hand side of Eq. (3.7) by its average with the GRFR pn QRPA vacuum state, denoted by

$$D_1(pn) = U_p^2 - U_n^2 + \frac{1}{2I_n + 1} (U_n^2 - V_n^2) \langle \hat{N}_n \rangle - \frac{1}{2I_p + 1} (U_p^2 - V_p^2) \langle \hat{N}_p \rangle. \quad (3.8)$$

The equations of motion show that the two qp energies are also renormalized:

$$E^{\text{ren}}(pn) = E_p(U_p^2 - V_p^2) + E_n(V_n^2 - U_n^2). \quad (3.9)$$

Here an important difference with respect to the FR pn QRPA equations should be pointed out. There, the quasiparticle energies defining the poles in the dispersion equation for the FR pn QRPA roots are of the types $E_p + E_n$ and $E_p - E_n$. They show up due to the commutation relations of the basic operators involved in the phonon operator with the independent quasiparticle term of the model Hamiltonian. The difference is caused by the gauge projection operation. The space of pn dipole states, \mathcal{S} , is written as a sum of three subspaces defined as

$$\begin{aligned} \mathcal{S}_+ &= \{(p, n) | D_1(pn) > 0, \quad E^{\text{ren}}(pn) > 0\}, \\ \mathcal{S}_- &= \{(p, n) | D_1(pn) < 0, \quad E^{\text{ren}}(pn) < 0\}, \\ \mathcal{S}_{\text{sp}} &= \mathcal{S} - (\mathcal{S}_+ + \mathcal{S}_-), \\ \mathcal{N}_{\pm} &= \dim(\mathcal{S}_{\pm}), \quad \mathcal{N}_{\text{sp}} = \dim(\mathcal{S}_{\text{sp}}), \\ \mathcal{N} &= \mathcal{N}_+ + \mathcal{N}_- + \mathcal{N}_{\text{sp}}. \end{aligned} \quad (3.10)$$

The fourth line here specifies the dimensions of these subspaces. In \mathcal{S}_+ one defines the renormalized operators

$$\begin{aligned}\bar{\mathcal{A}}_{1\mu}^\dagger(pn) &= \frac{1}{\sqrt{D_1(pn)}}\mathcal{A}_{1\mu}^\dagger(pn), \\ \bar{\mathcal{A}}_{1\mu}(pn) &= \frac{1}{\sqrt{D_1(pn)}}\mathcal{A}_{1\mu}(pn),\end{aligned}\quad (3.11)$$

while in \mathcal{S}_- the renormalized operators are

$$\begin{aligned}\bar{\mathcal{F}}_{1\mu}^\dagger(pn) &= \frac{1}{\sqrt{|D_1(pn)|}}\mathcal{A}_{1\mu}^\dagger(pn), \\ \bar{\mathcal{F}}_{1\mu}(pn) &= \frac{1}{\sqrt{|D_1(pn)|}}\mathcal{A}_{1\mu}^\dagger(pn).\end{aligned}\quad (3.12)$$

Indeed, the operator pairs $\mathcal{A}_{1\mu}, \mathcal{A}_{1\mu}^\dagger$ and $\mathcal{F}_{1\mu}, \mathcal{F}_{1\mu}^\dagger$ satisfy commutation relations of boson type. A pn QRPA treatment within \mathcal{S}_{sp} would yield either vanishing or negative energies. The corresponding states are therefore spurious. The FR pn QRPA with the gauge symmetry projected defines the phonon operator as

$$\Gamma_{1\mu}^\dagger = \sum_k [X(k)\bar{\mathcal{A}}_{1\mu}^\dagger(k) + Z(k)\bar{\mathcal{F}}_{1\mu}^\dagger(k) - Y(k)\bar{\mathcal{A}}_{1-\mu}(k)(-)^{1-\mu} - W(k)\bar{\mathcal{F}}_{1-\mu}(k)(-)^{1-\mu}]. \quad (3.13)$$

The summation in the defining equation (3.13) is restricted to the existence domain of the operators to which it is applied. Thus, when the term contains one of the operators $\bar{\mathcal{A}}_{1\mu}^\dagger(k), \bar{\mathcal{A}}_{1-\mu}(k)(-)^{1-\mu}$, then $k \in \mathcal{S}_+$. Also, for the terms

involving the operators $\bar{\mathcal{F}}_{1\mu}, \bar{\mathcal{F}}_{1\mu}^\dagger$ the summation is restricted to $k \in \mathcal{S}_-$.

The phonon amplitudes are determined by the equations

$$[H, \Gamma_{1\mu}^\dagger] = \omega\Gamma_{1\mu}^\dagger, \quad [\Gamma_{1\mu}, \Gamma_{1\mu'}^\dagger] = \delta_{\mu,\mu'}. \quad (3.14)$$

Thus, the phonon amplitudes are obtained by solving the GRFR pn QRPA equations

$$\begin{pmatrix} A_{11} & A_{12} & B_{11} & B_{12} \\ A_{21} & A_{22} & B_{21} & B_{22} \\ -B_{11} & -B_{12} & -A_{11} & -A_{12} \\ -B_{21} & -B_{22} & -A_{21} & -A_{22} \end{pmatrix} \begin{pmatrix} X(pn) \\ Z(pn) \\ Y(pn) \\ W(pn) \end{pmatrix} = \omega \begin{pmatrix} X(p_1n_1) \\ Z(p_1n_1) \\ Y(p_1n_1) \\ W(p_1n_1) \end{pmatrix}, \quad (3.15)$$

where the involved matrices are analytically given in the Appendix. In Ref. [16], the above equations were written in a compact form, under the form of a dispersion equation for the excitation energies. The phonon amplitudes were also analytically expressed.

The matrix dimension for A_{11} and B_{11} is $\mathcal{N}_+ \times \mathcal{N}_+$, while for A_{22} and B_{22} it is $\mathcal{N}_- \times \mathcal{N}_-$. The off diagonal submatrices A_{12} and B_{12} have the dimension $\mathcal{N}_+ \times \mathcal{N}_-$, while A_{21} and B_{21} are of the $\mathcal{N}_- \times \mathcal{N}_+$ type.

In order to solve Eqs. (3.15) we need to know $D_1(pn)$ and, therefore, the averages of the qp number operators \hat{N}_p and \hat{N}_n . These are written first in particle representation and then the particle-number-conserving term is expressed as a linear combination of $\mathcal{A}^\dagger\mathcal{A}$ and $\mathcal{F}^\dagger\mathcal{F}$ chosen such that their commutators with $\mathcal{A}^\dagger, \mathcal{A}$ and $\mathcal{F}^\dagger, \mathcal{F}$ are preserved. The final result is

$$\begin{aligned}\langle \hat{N}_p \rangle &= V_p^2(2I_p + 1) + 3(U_p^2 - V_p^2) \left(\sum_{\substack{n',k \\ (p,n') \in \mathcal{S}_+}} D_1(p, n') [Y_k(p, n')]^2 - \sum_{\substack{n',k \\ (p,n') \in \mathcal{S}_-}} D_1(p, n') [W_k(p, n')]^2 \right), \\ \langle \hat{N}_n \rangle &= V_n^2(2I_n + 1) + 3(U_n^2 - V_n^2) \left(\sum_{\substack{p',k \\ (p',n) \in \mathcal{S}_+}} D_1(p', n) [Y_k(p', n)]^2 - \sum_{\substack{p',k \\ (p',n) \in \mathcal{S}_-}} D_1(p', n) [W_k(p', n)]^2 \right).\end{aligned}\quad (3.16)$$

Equations (3.15), (3.16), and (3.8) are to be simultaneously considered and solved iteratively. It is worth mentioning that, by using the quasiparticle representation for the basic operators $\mathcal{A}_{1\mu}^\dagger, \mathcal{F}_{1\mu}^\dagger, \mathcal{A}_{1-\mu}(-)^{1-\mu}, \mathcal{F}_{1-\mu}(-)^{1-\mu}$ [see Eqs. (3.1), (3.11), and (3.12)], one obtains for $\Gamma_{1\mu}^\dagger$ an expression that involves the scattering pn operators. Thus, the present approach is, indeed, the GRFR pn QRPA.

IV. THE $2\nu\beta\beta$ PROCESS

The formalism presented above was used to describe the $2\nu\beta\beta$ process. If the energy carried by leptons in the intermediate state is approximated by the sum of the rest energy

of the emitted electron and half the Q value of the double- β decay process

$$\Delta E = \frac{1}{2}Q_{\beta\beta} + m_e c^2, \quad (4.1)$$

the reciprocal value of the $2\nu\beta\beta$ half-life can be factorized as

$$(T_{1/2}^{2\nu\beta\beta})^{-1} = F |M_{GT}(0_i^+ \rightarrow 0_f^+)|^2, \quad (4.2)$$

where F is an integral on the phase space, independent of the nuclear structure, while M_{GT} stands for the Gamow-Teller transition amplitude and has the expression

$$M_{GT} = \sqrt{3} \sum_{k,k'} \frac{i \langle 0 | \beta_i^+ | 1_k \rangle \langle 1_k | 1_{k'} \rangle_{ff} \langle 1_{k'} | \beta_f^+ | 0 \rangle_f}{E_k + \Delta E + E_{1+}}. \quad (4.3)$$

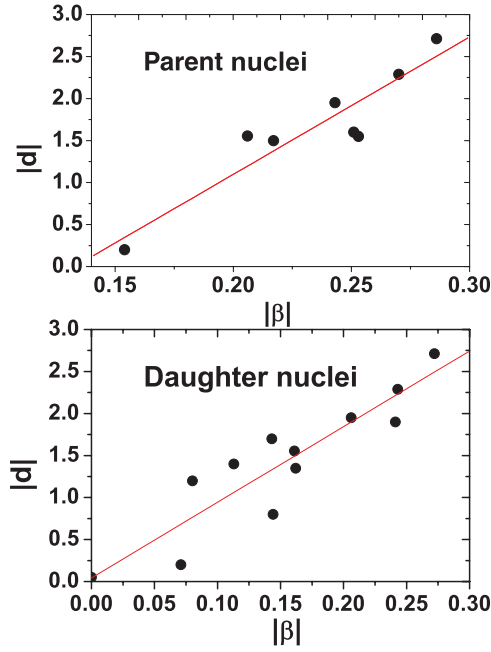


FIG. 2. (Color online) The relation between the deformation parameter d and the nuclear deformation β .

In this equation, the denominator consists of three terms: (i) ΔE , which was already defined, (ii) the average value of the k th GRFR pn QRPA energies in parent and daughter nuclei, respectively, normalized to the particular value corresponding to $k = 1$, and (iii) the experimental energy for the lowest 1^+ state. The indices carried by the β^+ operators indicate that they act in the space spanned by the GRFR pn QRPA states associated with the initial (i) or final (f) nucleus. The overlap MEs of the single-phonon states in the initial and final nuclei are calculated within the GRFR pn QRPA. In Eq. (4.3), the Rose convention for the reduced MEs is used [23].

Note that if we restrict the pn space to S_+ and, moreover, the dipole-pairing interaction is ignored, M_{GT} vanishes due to the second leg of the transition. Indeed, the ME associated with the daughter nucleus is of the type ${}_f\langle 0|(c_n^\dagger c_p)_{1\mu}(c_n^\dagger c_p)_{1\mu}|0\rangle_f$, which is equal to zero due to the Pauli principle restriction. In this case the equations of motion are of Tamm-Dankoff type and, therefore, the ground-state correlations are missing. In order to induce the necessary correlations we have either to extend the formalism in the space S_- , or to allow the p-h excitations to interact via a pairinglike force. Also, we remark that the operator $\bar{A}_{1\mu}^\dagger$ plays the role of a β^- transition operator, while when $\bar{F}_{1\mu}^\dagger$ or $A_{1\mu}$ is applied on the ground state of the daughter nucleus, it induces a β^+ transition. Therefore, the 2β decay cannot be described by considering the β^- transition alone.

V. NUMERICAL APPLICATION AND DISCUSSION

The approach presented in the previous sections was applied for the transitions of twelve double- β emitters: ^{48}Ca , ^{76}Ge ,

^{82}Se , ^{96}Zr , ^{104}Ru , ^{110}Pd , $^{128,130}\text{Te}$, $^{148,150}\text{Nd}$, ^{154}Sm , and ^{160}Gd . We present first the parameters involved in our calculations.

A. Parameters

The parameters defining the single-particle energies are those of the spherical shell model, the deformation parameter d and the parameter k relating the quadrupole coordinate with the quadrupole bosons, as shown in Eq. (2.2). These are fixed as described in Ref. [19]. As proved in Refs. [24,25], the parameter d and the nuclear deformation β are linearly related. This linear dependence is presented separately for parent and daughter nuclei in Fig. 2. Note that, except for ^{48}Ca and $^{128,130}\text{Te}$, all double- β emitters considered here are deformed. The daughter nuclei, except for ^{48}Ti , are also deformed. Moreover, the deformations characterizing the parent and daughter nuclei are different from each other. Actually these data justify the use of deformed single-particle states. While the core system energies depend quadratically on the deformation parameter d , the single-particle energies comprise a term linear in d due to the particle-core interaction. In this way energies corresponding to a negative d are associated with an oblate shape (see Fig. 1). For example, the deformation parameters of ^{104}Ru , $^{104,110}\text{Pd}$, and ^{110}Cd resulting from energy minimization are negative. On the other hand, according to Ref. [26] the isotopic chains $^{108-120}\text{Ru}$, $^{112-118}\text{Pd}$, and $^{112-118}\text{Cd}$ exhibit an oblate shape. It is worth mentioning that in Ref. [27] the predicted mass intervals for oblate shape are different from the ones mentioned above: $^{110-123}\text{Ru}$, $^{111-123}\text{Pd}$, and $^{115-119}\text{Cd}$. The reason is that they correspond to different mean fields. Since the mean fields used here differ from those of Refs. [26,27] the phase transition to the oblate shape takes place for a smaller atomic mass.

The proton and neutron pairing strengths are slightly different from those given in Ref. [19] since the dimension of the single-particle basis used in the present paper is different from that in Ref. [19].

The strength of the dipole pn two-body interaction was taken to be

$$\chi = \frac{5.2}{A^{0.7}} \text{ MeV}. \quad (5.1)$$

This expression was obtained by fitting the positions of the GT resonances in ^{40}Ca , ^{90}Zr , and ^{208}Pb [28]. The strength for the attractive pn two-body interaction was chosen so that the result for the $\log ft$ value associated with one of the single- β decays of the intermediate odd-odd nucleus was close to the corresponding experimental data. If the experimental data are missing, the restriction refers to the existing data in the neighboring region. The results for the fitted parameters are given in Table I. There we give also the result for the Ikeda sum rule.

The BCS calculations are performed by using a certain number of states outside an inert core. The core system for the 12 decays is defined by the (Z, N) , listed in Table II. Therein, one may find also the number of single-particle doubly degenerate states used in our calculations. In order to perform the GRFR pn QRPA calculation we have to divide the space of proton-neutron dipole states, S , into three subspaces

TABLE I. The deformation parameter d , the pairing interaction strengths for protons (G_p) and neutrons (G_n), and the GT dipole (χ) and dipole-pairing (X_{dp}) interaction strengths used in our calculations. We also give the parameter k relating the quadrupole coordinates and bosons (this is involved in the expression of the single-particle energies). Results for ISR/3 are to be compared with the corresponding $N - Z$ values.

	d	k	G_p (MeV)	G_n (MeV)	ISR/3	χ (MeV)	X_{dp} (MeV)
^{48}Ca	0.3	8	0.42	0.43	8.04	0.346	0.253
^{48}Ti	0.05	8	0.46	0.36	4.04	0.346	0.253
^{76}Ge	1.6	10	0.22	0.382	11.99	0.250	0.609
^{76}Se	1.9	10	0.24	0.325	7.99	0.250	0.609
^{82}Se	0.2	9	0.261	0.344	14.00	0.238	0.143
^{82}Kr	0.2	9	0.24	0.268	10.01	0.238	0.143
^{96}Zr	1.5	12	0.18	0.343	16.08	0.213	0.106
^{96}Mo	1.2	10	0.22	0.338	11.99	0.213	0.106
^{104}Ru	-1.55	12	0.18	0.35	16.00	0.201	0.502
^{104}Pd	-1.35	9	0.18	0.275	12.00	0.201	0.502
^{110}Pd	-1.6	10	0.16	0.306	18.05	0.194	0.775
^{110}Cd	-0.8	10	0.16	0.3105	13.97	0.194	0.775
^{128}Te	0.5	8	0.12	0.266	24.05	0.450	0.436
^{128}Xe	1.7	8	0.12	0.2518	20.02	0.450	0.436
^{130}Te	0.493	12	0.10	0.292	26.00	0.7	0.840
^{130}Xe	1.4	12	0.11	0.286	21.94	0.7	0.840
^{148}Nd	1.555	14	0.11	0.2516	28.02	0.157	0.142
^{148}Sm	1.555	14	0.11	0.225	24.04	0.157	0.142
^{150}Nd	1.952	16	0.10	0.254	30.05	0.156	0.016
^{150}Sm	1.952	16	0.11	0.235	26.08	0.156	0.016
^{154}Sm	2.29	16	0.10	0.316	30.08	0.153	0.138
^{154}Gd	2.29	14	0.11	0.27	26.01	0.153	0.138
^{160}Gd	2.714	10	0.11	0.3	32.07	0.149	0.298
^{160}Dy	2.714	8	0.11	0.2578	28.02	0.149	0.298

(\mathcal{S}_+ , \mathcal{S}_- , \mathcal{S}_{sp}), according to the definition given by Eq. (3.10). The dimensions for the spaces (\mathcal{S}_+ , \mathcal{S}_- , \mathcal{S}) for the parent (D_1) and daughter (D_2) nuclei are also listed. As explained in the previous sections, the GRFR pn QRPA equations together with the constraint equations are to be solved iteratively. In Table II, we give the number of iterations that are necessary in order to achieve the process convergence.

B. Single- β transition strengths $B(\text{GT}^\pm)$

Since the double- β matrix elements are expressed as a product of two reduced matrix elements, one associated with the β^- transition of the parent nucleus and the second one with the β^+ transition of the daughter nucleus, it is worthwhile to study the strength distribution over the GRFR pn QRPA energies, for the two transitions.

TABLE II. The number of single-particle proton states lying above the (Z, N) core is given. The single-particle space for neutrons is identical to that for protons. D_1 and D_2 are the dimensions of the spaces \mathcal{S}_+ , \mathcal{S}_- , \mathcal{S} defined in the text, for the parent and daughter nuclei, respectively. The dimension of the GRFR pn QRPA matrix is equal to the sum of the \mathcal{S}_+ and \mathcal{S}_- dimensions. Also, the number of steps necessary for the iterative procedure convergence is listed.

Nucleus	Core's (Z, N)	Number of states	D_1	D_2	Number of iterations
^{48}Ca	(0,0)	31	(96,0,103)	(79,7,103)	7
^{76}Ge	(20,20)	31	(96,0,119)	(83,0,119)	5
^{82}Se	(20,20)	37	(107,0,135)	(95,0,135)	4
^{96}Zr	(20,20)	39	(116,0,141)	(105,8,141)	15
^{104}Ru	(26,26)	39	(118,1,140)	(111,2,140)	7
^{110}Pd	(26,26)	43	(146,0,162)	(125,7,162)	6
^{128}Te	(28,28)	60	(191,0,228)	(185,1,232)	5
^{130}Te	(42,42)	67	(204,0,242)	(182,0,244)	6
^{148}Nd	(40,40)	51	(158,3,203)	(168,1,203)	5
^{150}Nd	(40,40)	57	(203,2,246)	(197,1,246)	4
^{154}Sm	(40,40)	57	(203,0,249)	(204,3,249)	9
^{160}Gd	(40,40)	59	(216,1,253)	(215,0,253)	14

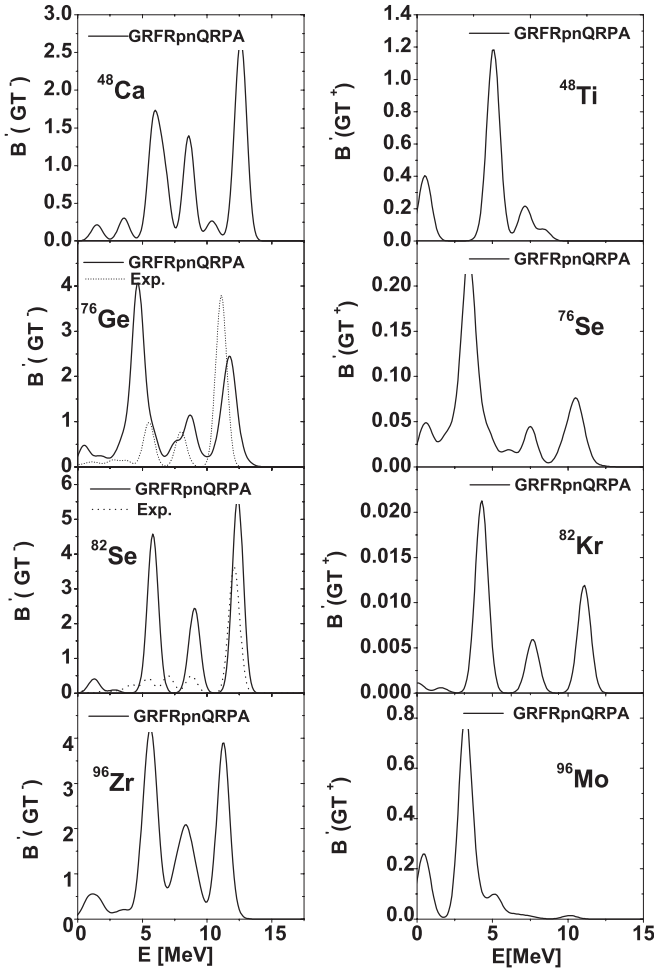


FIG. 3. One-third of the single- β^- (left column) and one-third of the β^+ (right column) strengths, denoted by $B'(GT^-)$ and $B'(GT^+)$, for the parent, ^{48}Ca , ^{76}Ge , ^{82}Se , and ^{96}Zr , and daughter, ^{48}Ti , ^{76}De , ^{82}Kr , and ^{96}Mo , nuclei, respectively, folded with a Gaussian function with a width of 1 MeV, are plotted as functions of the corresponding energies yielded by the present formalism. Note that the difference of the two strengths for the parent nucleus should amount to $N - Z$ if the sum rule is obeyed. For ^{76}Ge and ^{82}Se , the experimental data for the β^- strength are also presented.

Using the data shown in Tables I and II as input, we calculated the distribution of the β^\pm strengths with the results shown in Figs. 3–5. The energy intervals where both strengths are large contribute significantly to the double- β transition amplitude. The β^- strength is fragmented among the GRFRpnQRPA states, reflecting the fact that the single-particle states are deformed. The β^- strengths for the emitters considered in Fig. 3 exhibit three major peaks. ^{48}Ca and ^{76}Ge each have one additional small bump close to the last and intermediate major peaks, respectively. The β^- strength of ^{48}Ca has been studied in Ref. [29] where the GT resonance was populated in the reaction $^{48}\text{Ca}(p, n)^{48}\text{Sc}$. It was shown that the GT resonance is spread over an energy interval between 4.5 and 14.5 MeV. As seen from Fig. 3, the results of our calculations concerning the width of the GT resonance agree with the mentioned experimental data. In ^{76}Ge and ^{82}Se the strength

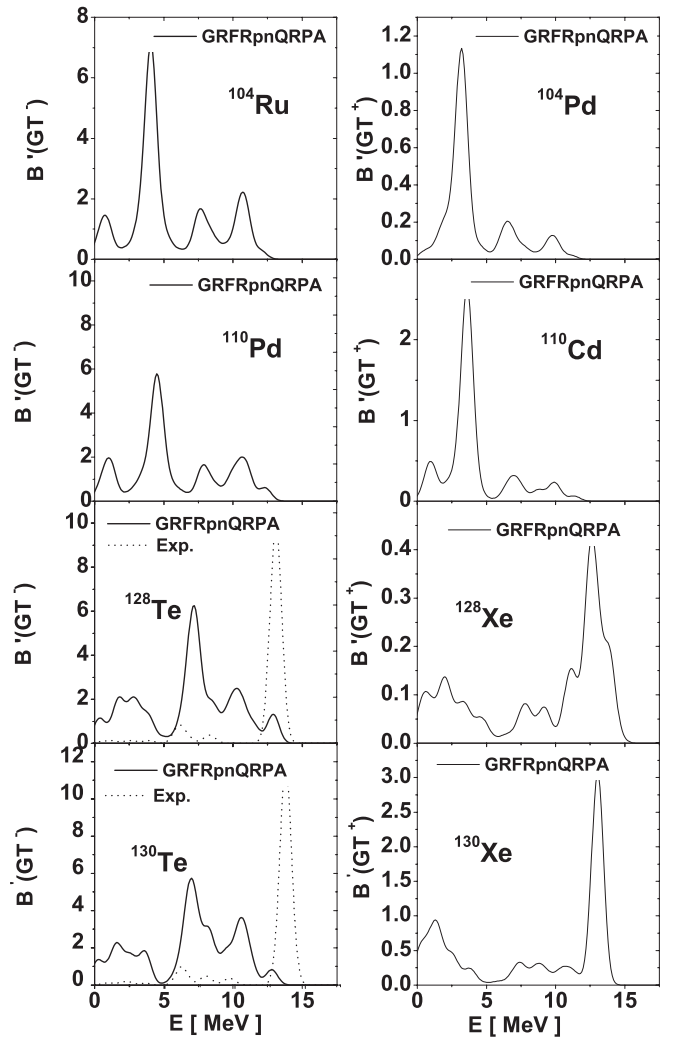


FIG. 4. As Fig. 3 but for the parent nuclei ^{104}Ru , ^{110}Pd , and $^{128,130}\text{Te}$ and the daughter nuclei ^{104}Pd , ^{110}Cd , and $^{128,130}\text{Xe}$, respectively. For $^{128,130}\text{Te}$, the experimental data are also presented.

distribution has been studied in the reactions $^{76}\text{Ge}(p, n)^{76}\text{As}$ and $^{82}\text{Se}(p, n)^{82}\text{Br}$ [30], respectively. The $B(GT)$ values have been extracted from the excitation energy spectrum. These values have been folded with a Gaussian with a width of 1 MeV and plotted in Fig. 3 to be compared with the results of our calculation. We notice that the centroids of the large peaks from ^{76}Ge lie close to those shown by the experimental data. Concerning ^{82}Se , the large peak is nicely described. The centroids of the two smaller peaks lie close to the peaks predicted by our calculations. It is worth mentioning that it is hard to make a fair comparison between the magnitudes of the peaks in our calculations and those extracted from the experimental data. Indeed, the total experimental $B'(GT^-)$ strengths for ^{76}Ge and ^{82}Se represent only 65% and 59% respectively, of the $(N - Z)$ value [30]. We notice that the β^- strength has a little bump below 2.5 MeV which is specific to the fully renormalized formalism, this strength being carried by the amplitude of the scattering terms. The new terms in the phonon operator are shown even more clearly in the β^+ strength where in three cases a peak close to zero shows up.

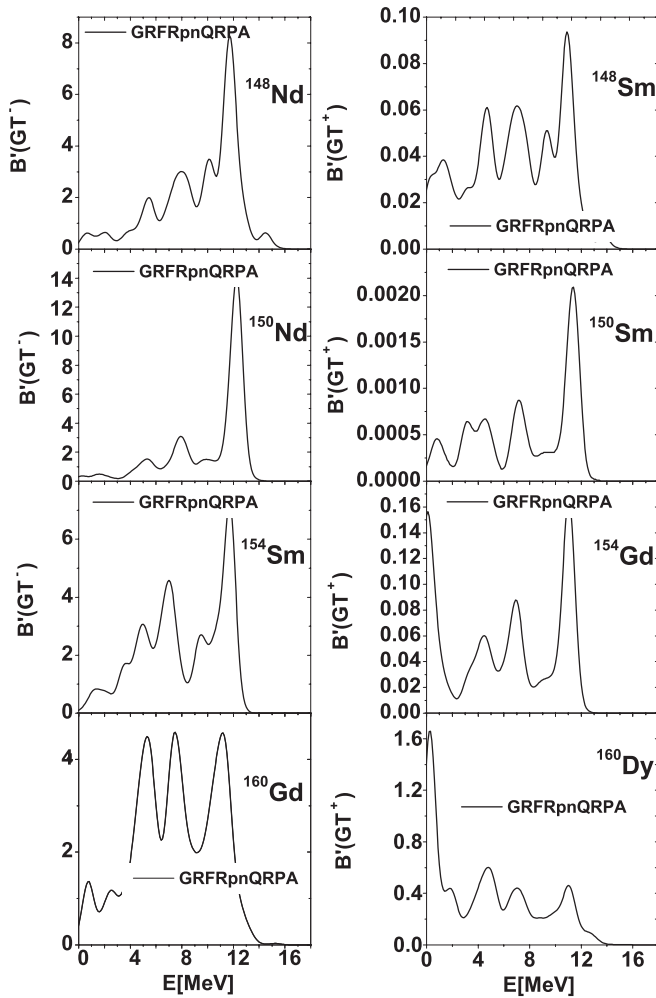


FIG. 5. As Fig. 3 but for the parent nuclei $^{148,150}\text{Nd}$, ^{154}Sm , and ^{160}Gd and the daughter nuclei $^{148,150}\text{Sm}$, ^{154}Gd , and ^{160}Dy , respectively.

Note that, while in the β^- case there is no strength beyond the last major peak, for the β^+ case small peaks show up after the major peak. This feature is most evident in ^{76}Se and ^{82}Kr . Because of the overlap of their energy spread with that of the major peak in the distribution of the β^- strength, they contribute significantly to the GT transition amplitude.

The β^- strengths shown in Fig. 4 exhibit some specific features. ^{104}Ru and ^{110}Pd have a low-energy peak centered at about 1 MeV, while the GT resonance (GTR) is spread over a wide interval ranging from 2.5 to 12.8 MeV with the strength shared mainly by three peaks. The β^- strength distributions for ^{128}Te and ^{130}Te start with a wide peak spread over the interval 0 to 5 MeV and continue with the GTR located between 5 and 14 MeV. The experimental β^- strengths for these nuclei were extracted from the excitation energy spectrum at 0.3° and 134.4 MeV, measured in the reactions $^{128}\text{Te}(p,n)^{128}\text{I}$ and $^{130}\text{Te}(p,n)^{130}\text{I}$, respectively [30]. Our calculations confirm the three-peak and four-peak structures in the two nuclei. However, the highest peak in our calculations is the first one, while the experimental dominant peak is the last one, located at 13.14 MeV in ^{128}Te and 13.59 MeV in ^{130}Te [30]. Also,

we note that the theoretical peaks are not sharply separated as suggested by the experimental data after elimination of the background contribution to the GTR.

Again, the relevance of comparing the results with the corresponding experimental data is dictated by the fact that the total experimental $B'(\text{GT}^-)$ strengths for ^{128}Te and ^{130}Te , accounting also for the contribution of the background, represent only 72% and 71% respectively, of the $(N - Z)$ value [30]. If the background contribution to the total strength is eliminated, as happens in Fig. 4, the total measured strength amounts to about 56% and 59%, respectively. The β^- strength seen below 2.5 MeV, which is specific to the fully renormalized formalism, seems to be carried by the amplitude of the scattering terms. The new terms in the phonon operator are manifest also in the β^+ strength distribution, where in three cases a peak close to zero shows up. While for the first two nuclei the dominant peaks in the β^+ strength are in the low-energy region for the two isotopes of Te the peak centroid energies are almost identical to the corresponding GTR centroid energies.

What might be the origin of the discrepancy between the theoretical and experimental β^- strengths for $^{128,130}\text{Te}$? In what follows we attempt to answer this question by commenting on some relevant features. In Ref. [31], Zamick and Auerbach explained the large decay rate of ^{76}Ge by the fact that the contributions from different shell transitions add coherently because the matrix elements of the interaction operator have the same sign. However, a destructive effect may appear due the mixing of the intermediate states or due to the four-quasiparticle admixture in the ground state [32]. In our formalism both situations occur, which results in having a maximal effect for $^{128,130}\text{Te}$ where the GT resonance is very much diminished. Perhaps this picture will change if a better algorithm for fixing the strength of the attractive interaction is found. A similar situation appeared when the dipole-dipole interaction was simultaneously considered in the p-h and p-p channels. Indeed, the GT transition amplitude is very sensitive to changes in the p-p interaction strength. Therefore to increase the predictive power of the formalism a method of fixing this strength was necessary. In Refs. [33,34] it was fixed by the constraint of minimizing the β^+ transition strength. For this value, within the $pn\text{QRPA}$ formalism, the isospin and Wigner SU(4) symmetries are maximally restored. When these symmetries are valid the GT resonance consists of one collective state, and the β^+ strength is equal to zero, which is a specific feature of the strong-coupling limit. However, for deformed nuclei, as are most of decaying isotopes considered here, the two symmetries are broken both by the adopted approximations (like the BCS approximation) and the nuclear deformation. Although the attractive pn interactions used here and in Ref. [34] are different from each other, we notice that the shape of the β^- strength obtained here is similar to that from Ref. [34] in the unperturbed limit of the transition operator. However, since the dipole-pairing interaction is attractive there is a critical value where one solution of the $pn\text{QRPA}$ equation is vanishing. The corresponding phonon operator becomes Hermitian and cannot be normalized to unity. Moreover, it plays the role of a symmetry generator. In the case of the Fermi interaction this symmetry expresses the invariance against any

rotation around the OX axis in the isospin space. This symmetry shows up as a signature of the breaking down of the $pnQRPA$ approach and reflects a phase transition of the nucleon system. For the critical value of the attractive interaction the strength for the β^+ transition of the daughter nucleus vanishes. The β^- strength of the parent nucleus is, however, different from zero (the breakdown of the $pnQRPA$ in the parent nucleus takes place for a larger interaction strength than in the daughter nucleus) and not concentrated in a single state. This critical behavior can be avoided by choosing the mean field to be consistent with the attractive proton-neutron interaction. In Ref. [35] this feature was studied for the Fermi interaction and, indeed, the first $pnQRPA$ root plotted as a function of the p-p interaction strength is not vanishing but has a minimum value which corresponds to a minimum value of the β^+ decay strength of the daughter nucleus. Another issue related to our treatment is the fact that the Fermi transitions are ignored. This hypothesis is only approximately valid, and moreover the position of the isobar analog state is about the same as that of the GT resonance. This suggests that a way to improve the description of the single- β^- GT transition strength would be to find a better way of fixing the strength of the attractive interaction strength and to simultaneously treat the GT and Fermi transitions.

The β^- strength distributions for the double- β emitters $^{148,150}\text{Nd}$, ^{154}Sm , and ^{160}Gd are presented in Fig. 5. For the first two transitions the β^- strength has a dominant peak, which is just the GT resonance. For ^{154}Sm and ^{160}Gd , one and two additional peaks show up at lower energy and with heights comparable to that of the GT resonance. The β^+ strength is also fragmented but exhibits a single dominant peak located at an energy close to the GT resonance centroid. For the transitions of ^{154}Gd and ^{160}Dy , an important amount of strength is accumulated in the low part of the spectrum. Actually this appears to be an effect caused by the scattering terms from the phonon operator.

As seen from Table I the results of our calculations for single- β transition strengths obey the ISR.

An interesting result that is worth mentioning concerns the summed strength for the β^- and β^+ transitions, denoted conventionally by $\sum B(GT^-)$ and $\sum B(GT^+)$, respectively.

TABLE III. The calculated summed strengths for the β^- strength associated with the parent nuclei and the summed β^+ strengths for the daughter nuclei, quenched by a factor of 0.6, are compared with the corresponding available data.

Nucleus	$0.6\sum B(GT)^-$	$\sum[B(GT)^-]_{\text{expt}}$	Nucleus	$0.6\sum B(GT)^+$	$\sum[B(GT)^+]_{\text{expt}}$
^{48}Ca	14.54	14.4 ± 2.5 [38]	^{48}Ti	3.666	1.9 ± 0.5 [38]
^{76}Ge	23.037	23.3 [30]	^{76}Se	1.125	1.45 ± 0.07 [36]
^{82}Se	25.372	24.6 [30]	^{82}Kr	0.079	
^{96}Zr	29.163		^{96}Mo	2.537	0.29 ± 0.08 [37]
^{104}Ru	32.921		^{104}Pd	3.990	
^{110}Pd	32.932		^{110}Cd	7.239	
^{128}Te	43.485	40.08 [30]	^{128}Xe	2.917	
^{130}Te	47.432	45.90 [30]	^{130}Xe	13.040	
^{148}Nd	51.74		^{148}Sm	1.29	
^{150}Nd	54.11		^{150}Sm	0.02	
^{154}Sm	54.68		^{154}Gd	0.54	
^{160}Gd	57.93		^{160}Dy	0.21	

These single- β decay strengths quenched with a factor of 0.6 [31], accounting for the polarization effects on the single- β transition operator, ignored in the present paper, are listed in Table III. Actually, the quenched values are to be compared with the experimental data, since the measured $B(GT)$ strength represents about 60–70% of the strength corresponding to the ISR.

The experimental value for the summed $B(GT^-)$ of ^{48}Ca is taken from Ref. [38], where from the total strength, which amounts to about 15.3 ± 2.2 , the contribution of isovector spin monopole states was extracted. The result was obtained with the reaction $^{48}\text{Ca}(p,n)^{48}\text{Sc}$, and corresponds to a large energy excitation interval, from 0 to 30 MeV.

In Ref. [30] the total GT strength, for ^{76}Ge and ^{82}Se consists of the sum of the strength observed in the peaks plus the estimated contribution from the background. The experimental results correspond to 65% and 59% of the $3(N - Z)$ sum rule. According to Ref. [29], by adding to the GT cross section in discrete states the contribution from the background and that of the continuum, the total strength magnitude is much improved and better obeys the sum rule. We note a good agreement between the results of our calculations for the summed β^- strength and the corresponding experimental data.

The experimental data for the summed $B(GT^+)$ transition of ^{48}Ti were taken from Ref. [38]. This result was obtained after extracting the contribution of the isovector spin monopole states from the total strength of 2.8 ± 0.3 . The reaction $^{48}\text{Ti}(n,p)^{48}\text{Sc}$ was used to study the $B(GT^+)$ strength for excitation energies up to 30 MeV. This value for the total strength is larger than that reported by Alford *et al.*, in Ref. [39],

$$\sum B(GT^+) = 1.42 \pm 0.2, \quad (5.2)$$

where only the contributions of states with excitation energies up to 15 MeV are taken into account. This comparison shows that, indeed, the $B(GT)$ strength is sensitive to the magnitude of the considered energy interval. In this context we mention the results obtained through the charge exchange reactions ($^3\text{He},t$) and ($d,^2\text{He}$) on ^{48}Ca and ^{48}Ni , respectively [40], for $B(GT^-)$ and $B(GT^+)$ with an excitation energy interval $E_x \leq 5$ MeV: 1.43(38) and 0.45.

The GT strength from the $^{76}\text{Se}(n, p)^{76}\text{As}$ reaction [36] is 1.45 ± 0.07 and corresponds to an excitation energy $E_x \leq 10$ MeV. The authors used the multipole decomposition method. In Ref. [41] the $B(\text{GT}^+)$ strength was measured in a different reaction, $^{76}\text{Se}(d, ^2\text{He})^{76}\text{As}$, and a different excitation energy interval, $E_x \leq 4$ MeV. The result reported is $\sum_{0-4 \text{ MeV}} B(\text{GT}^+) = 0.54 \pm 0.1$, which is smaller than that from Ref. [36]. The length of the energy intervals justifies the mentioned differences. We remark that the results for the summed β^+ strength in ^{48}Ti and ^{76}Se are in reasonably good agreement with the corresponding experimental data.

The last strength mentioned in Table III refers to the daughter nucleus ^{96}Mo . Through the reaction $^{96}\text{Mo}(d, ^2\text{He})^{96}\text{Nb}$ the strength taken mainly by a single state, placed at 0.69 MeV, was measured. However, from Fig. 3 we note that, indeed, there is a state at 0.69 MeV which catches a certain β^+ strength, but that strength is smaller than that distributed among the states lying in the energy interval of 1.8 to 7.5 MeV. More complete measurement through a (p, n) reaction on ^{96}Mo and an energy range of 0–10 MeV is necessary in order to make a fair comparison with the results presented here.

The quenched values of the total β^- strength of $^{128,130}\text{Te}$ are compared with the experimental data since the measured $B(\text{GT}^-)$ strength, as we mentioned before, represents about 56% and 59%, respectively, of the strength corresponding to the ISR. There are some claims [29] that addition of the strength carried by the states from the continuum corrects the total $B(\text{GT})$ strength to 90% of the simple sum rule result. We remark the good agreement between the calculated and experimental total strengths. Note that if we replaced the quenching factor by 0.56 for ^{128}Te and by 0.59 for ^{130}Te , the results for the total strength would be 40.586 and 46.56, respectively, which are closer to the experimental data. Unfortunately for the last four parent and the last four daughter nuclei, there are no data available for the single- β^- and single- β^+ strengths, respectively.

C. Transition amplitude and half-life

The energy corrections involved in Eq. (4.3) for the considered double- β emitters are

$$\begin{aligned} \Delta E(^{48}\text{Ca}) &= 2.646 \text{ MeV}, & E_{1+}(^{48}\text{Sc}) &= 0.338 \text{ MeV}, \\ \Delta E(^{76}\text{Ge}) &= 1.530 \text{ MeV}, & E_{1+}(^{76}\text{As}) &= 0.044 \text{ MeV}, \\ \Delta E(^{82}\text{Se}) &= 2.016 \text{ MeV}, & E_{1+}(^{82}\text{Br}) &= 0.075 \text{ MeV}, \\ \Delta E(^{96}\text{Zr}) &= 2.186 \text{ MeV}, & E_{1+}(^{160}\text{Nb}) &= 1.116 \text{ MeV}, \\ \Delta E(^{104}\text{Ru}) &= 1.161 \text{ MeV}, & E_{1+}(^{104}\text{Rh}) &= 0.0 \text{ MeV}, \\ \Delta E(^{104}\text{Pd}) &= 1.516 \text{ MeV}, & E_{1+}(^{110}\text{Ag}) &= 0.0 \text{ MeV}, \\ \Delta E(^{128}\text{Te}) &= 0.946 \text{ MeV}, & E_{1+}(^{128}\text{I}) &= 0.58 \text{ MeV}, \\ \Delta E(^{130}\text{Te}) &= 1.776 \text{ MeV}, & E_{1+}(^{130}\text{I}) &= 0.85 \text{ MeV}, \\ \Delta E(^{148}\text{Nd}) &= 1.476 \text{ MeV}, & E_{1+}(^{148}\text{Pm}) &= 0.137 \text{ MeV}, \\ \Delta E(^{150}\text{Nd}) &= 2.196 \text{ MeV}, & E_{1+}(^{150}\text{Pm}) &= 0.137 \text{ MeV}, \\ \Delta E(^{154}\text{Sm}) &= 1.530 \text{ MeV}, & E_{1+}(^{154}\text{Eu}) &= 0.046 \text{ MeV}, \\ \Delta E(^{160}\text{Gd}) &= 0.046 \text{ MeV}, & E_{1+}(^{160}\text{Tb}) &= 0.139 \text{ MeV}. \end{aligned}$$

(5.3)

Calculating first the GT transition amplitude and then the Fermi integral with $G_A = 1.254$, as in Ref. [4], we obtained the half-lives given in Table IV. There we also give the experimental data taken from different sources as well as the results obtained by other procedures. From there one can see that the results of our calculations agree quite well with the corresponding experimental data. The results of Ref. [10] were obtained within a standard renormalized pn QRPA formalism and therefore the ISR is violated.

D. Transitions of the intermediate odd-odd nucleus

The intermediate odd-odd nuclei involved in the double- β process can, in principle, perform the transition β^+ or electron capture (EC), which results in feeding the parent nucleus of each transition. On the other hand, they can perform a β^- transition to the corresponding daughter nuclei. For some transitions of this type the $\log ft$ values have been measured. The corresponding theoretical results are obtained by means of the expression

$$ft_{\mp} = \frac{6160}{[l \langle 1_1 || \beta^{\pm} || 0 \rangle_{l g_A}]^2}, \quad l = i, f. \quad (5.4)$$

In order to take account of the effect of distant states responsible for the “missing strength” in the giant GT resonance [4] we chose $g_A = 1.0$. In a previous publication [19], where a standard pn QRPA approach was used, the strengths of the p-h and p-p interactions were fixed in order to reproduce the $\log ft$ values characterizing the two transitions of the intermediate odd-odd nucleus. Similarly, here the strengths of the two-body proton-neutron interactions, χ and X_{dp} , could be fixed by fitting the $\log ft$ values associated with the two single- β transitions. Unfortunately, there are not enough available data to enable a fitting procedure. In Table V the results of our calculations for the mentioned $\log ft$ values are listed.

Due to the lack of experimental data for this single- β decay strength, the strength of the p-h interaction was taken as given by Eq. (5.1). However, as seen from Fig. 3 the predicted centroid of the GT resonance has a small shift with respect to the experimental one. This suggests that Eq. (5.1) should be reconsidered and the fit of the GT resonance centroids be performed within the GRFR pn QRPA. Actually, the strength of the attractive pn dipole-pairing interaction was chosen such that one of the decay branches of the odd-odd nuclei has a $\log ft$ value close to those known for the chosen nucleus or for a nucleus from the neighboring region.

E. Previous consideration of the subject

After our paper on fully renormalized pn QRPA was published [11], another approach addressing the same issue showed up [22,60], which suggests that the results obey the ISR. However as pointed out in Ref. [61], that formalism does not satisfy the consistency condition required by the linearization procedure. Actually, this feature was outlined in Sec. III of the present paper. Indeed, we showed that within the linearization procedure framework, the p-p interaction term does not contribute to the equations of motion if the

TABLE IV. The Gamow-Teller amplitude for the $2\nu\beta\beta$ decay, in units of MeV^{-1} , and the corresponding half-life ($T_{1/2}$), in units of yr, are listed for 12 ground-to-ground transitions. The experimental half-lives for the transitions were taken from the specified references. Comparison is also made with the theoretical results from the last three columns, reported in Refs. [18,19], [42–44], and [10,45], respectively.

	M_{GT} (MeV^{-1})	$T_{1/2}$ (yr)				
		Present	Expt.	Raduta <i>et al.</i> [18,19]	Klapdor <i>et al.</i> [42–44]	Others [10,45]
$^{48}\text{Ca} \rightarrow ^{48}\text{Ti}$	0.045	4.72×10^{19}	$(4.2 \pm 1.2) \times 10^{19}$ [46] $4.4_{-0.5}^{+0.6} \times 10^{19}$ [47]	7.48×10^{19}	3.2×10^{19}	
$^{76}\text{Ge} \rightarrow ^{76}\text{Se}$	0.177	0.938×10^{21}	$9.2_{-0.4}^{+0.7} \times 10^{20}$ [48] $(1.5 \pm 0.1) \times 10^{21}$ [47]	4.05×10^{20}	2.61×10^{20}	1.4×10^{21} [10]
$^{82}\text{Se} \rightarrow ^{82}\text{Kr}$	0.083	1.293×10^{20}	$1.1_{-0.3}^{+0.8} \times 10^{20}$ [49] $(0.92 \pm 0.07) \times 10^{20}$ [47]	0.963×10^{20}	0.848×10^{20}	1.1×10^{20} [10]
$^{96}\text{Zr} \rightarrow ^{96}\text{Mo}$	0.115	1.59×10^{19}	$(1.4_{-0.5}^{+3.5}) \times 10^{19}$ [50] $(2.3 \pm 0.2) \times 10^{19}$ [47]	0.44×10^{19}	5.2×10^{17}	4.4×10^{19} [10]
$^{104}\text{Ru} \rightarrow ^{104}\text{Pd}$	0.453	2.26×10^{21}		0.76×10^{21}	1.8×10^{21} 3.1×10^{22}	
$^{110}\text{Pd} \rightarrow ^{110}\text{Cd}$	0.188	3.11×10^{20}		1.58×10^{20}	5.0×10^{19} 1.2×10^{21}	
$^{128}\text{Te} \rightarrow ^{128}\text{Xe}$	0.056	1.43×10^{24}	$(7.2 \pm 0.3) \times 10^{24}$ [50] $(1.5 \pm 0.2) \times 10^{24}$ [51] $(1.9 \pm 0.4) \times 10^{24}$ [47]	0.55×10^{24}	1.2×10^{23} 5.7×10^{23}	5.6×10^{23} [10]
$^{130}\text{Te} \rightarrow ^{130}\text{Xe}$	0.023	1.56×10^{21}	$(1.5-2.8) \times 10^{21}$ [50] $(2.7 \pm 0.1) \times 10^{21}$ [51] $(0.7 \pm 0.3) \times 10^{21}$ [53] $(6.8_{-1.1}^{+1.2}) \times 10^{20}$ [47]	0.26×10^{21}	1.9×10^{19} 1.2×10^{20}	0.26×10^{21} [10]
$^{148}\text{Nd} \rightarrow ^{148}\text{Sm}$	0.422	2.00×10^{19}		2.33×10^{19}	1.19×10^{21}	
$^{150}\text{Nd} \rightarrow ^{150}\text{Sm}$	0.042	2.50×10^{19}	$\geq 1.8 \times 10^{19}$ [54] $(1.7_{-0.6}^{+1.1}) \times 10^{19}$ [55] $(8.2 \pm 0.9) \times 10^{18}$ [47]	2.63×10^{17}	1.66×10^{19}	6.7×10^{19} [45]
$^{154}\text{Sm} \rightarrow ^{154}\text{Gd}$	0.303	2.02×10^{21}		8.76×10^{20}	1.49×10^{22}	
$^{150}\text{Gd} \rightarrow ^{150}\text{Dy}$	0.111	1.02×10^{21}		2.013×10^{20}	2.81×10^{21}	

condition of conserving the nucleon total number holds. However, in Refs. [22,60] the p-p interaction influence on the phonon amplitudes is taken into account by averaging some specific double commutators on the vacuum state. If the same path is followed for the number-nonconserving terms, their amplitudes in the phonon operator cannot vanish. According to Ref. [60], the experimental GT transition amplitude is reached for a p-p interaction strength close to the breakdown value of the pn QRPA. Moreover, the breakdown point of the fully renormalized pn QRPA lies close to and below the breakdown point of the standard pn QRPA. This result is on a par with our result from Ref. [11]. Therefore even if the ISR is satisfied, the principal problem of having a stable ground state for the parent and daughter nuclei still persists.

An attractive interaction of p-h dipole-pairing type is responsible for the ground-state correlations. To a lesser extent these are also caused by the \mathcal{F} components of the new phonon operator. Projection of the gauge is essential for restoring the ISR. Gauge projection of the pn QRPA was previously achieved in Ref. [62] where the ISR was satisfied in any case within the unprojected picture. By contrast, there the effect of projection was small.

Generally speaking, whenever some conditions, like full renormalization and gauge symmetry restoration, are met a certain price is expected to be paid. Thus, there are some specific weak points that require further improvements. Indeed, the average of the quasiparticle number operators has been approximately calculated. We feel that a better expression can be found for this quantity, which is essential for the adopted iterative procedure. We hope that a better representation for the average number of quasiparticles will speed up the convergence of the iterative process. Moreover, this will allow us to extend our calculations to heavier nuclei. The renormalized vacuum state is characterized by a nonvanishing average number of quasiparticles. That means that the pn QRPA features are determined by the pairing properties not only through the occupation probabilities U^2 and V^2 but also by the averages of the quasiparticle number operators. The question that arises is whether the pn QRPA may influence the pairing properties. A positive answer could supply us with a unifying variational principle for both the vacua of quasiparticles and pn QRPA bosons. This goal was in fact touched on within a different context by Jolos and Rybarska-Nawrocka [63]. These features concerning the description of

TABLE V. The $\log ft$ values characterizing the β^+ or EC and β^- processes associated with the intermediate odd-odd nuclei are listed.

Parent nucleus		Odd-odd nucleus		Daughter nucleus
^{48}Ca	β^+ or EC \longleftarrow	^{48}Sc	β^- \longrightarrow	^{48}Ti
Theory	8.44		4.63	
^{76}Ge	β^+ or EC \longleftarrow	^{76}As	β^- \longrightarrow	^{76}Se
Theory	4.57		6.13	
^{82}Se	β^+ or EC \longleftarrow	^{82}Br	β^- \longrightarrow	^{82}Kr
Theory	8.11		7.18	
^{96}Zr	β^+ or EC \longleftarrow	^{96}Nb	β^- \longrightarrow	^{96}Mo
Theory	5.67		7.00	
^{104}Ru	β^+ or EC \longleftarrow	^{104}Rh	β^- \longrightarrow	^{104}Pd
Expt.	4.32 [56]		4.55 [56]	
Theory	4.71		6.47	
^{110}Pd	β^+ or EC \longleftarrow	^{110}Ag	β^- \longrightarrow	^{110}Cd
Expt.	4.08 [57]		4.66 [57]	
Theory	4.14		6.32	
^{128}Te	β^+ or EC \longleftarrow	^{128}I	β^- \longrightarrow	^{128}Xe
Expt.	5.049 [58]		6.061 [59]	
Theory	5.87		6.06	
^{130}Te	β^+ or EC \longleftarrow	^{130}I	β^- \longrightarrow	^{130}Xe
Theory	6.08		5.80	
^{148}Nd	β^+ or EC \longleftarrow	^{148}Pm	β^- \longrightarrow	^{148}Sm
Theory	6.8		7.33	
^{150}Nd	β^+ or EC \longleftarrow	^{150}Pm	β^- \longrightarrow	^{150}Sm
Theory	5.55		8.46	
^{154}Sm	β^+ or EC \longleftarrow	^{154}Eu	β^- \longrightarrow	^{154}Gd
Theory	5.52		5.13	
^{160}Gd	β^+ or EC \longleftarrow	^{160}Tb	β^- \longrightarrow	^{160}Dy
Theory	5.25		4.20	

the quasiparticle number operators in a better way as well as of the BCS and the pn QRP approximations in a unified fashion by a set of coupled equations derived from a unique variational principle will be implemented in a subsequent presentation.

The present formalism was recently applied for describing the double- β decay for ^{100}Mo and ^{116}Cd [15,16]. The positive results obtained there encouraged us to continue the investigation of double- β processes for other nuclei. As mentioned before, the strength of the attractive two-body pn interaction is fixed in a different manner here than in Refs. [15,16]. Moreover the single-particle space dimensions are different, which results in different pairing properties and quasiparticle correlations.

VI. CONCLUSIONS

Summarizing the results of this paper, one may say that restoration of the gauge symmetry from the fully renormalized pn QRP provides a consistent and realistic description of the

transition rate and, moreover, the ISR is obeyed. As shown in this paper, it seems that there is no need to include the p-p interaction in the many-body treatment of the process. Indeed, in the framework of a pn QRPA approach, this interaction violates the total number of particles and consequently the gauge projection process makes it ineffective. The proton-neutron correlations in the ground state are, however, determined by an attractive dipole-pairing interaction. The results of our calculations are compared with those obtained by different methods as well as with the available experimental data. Here the strength of the p-h interaction was taken as given by Eq. (5.1), while the one for the dipole-pairing interaction was approximately fixed such that one decay branch of the intermediate odd-odd nucleus has a $\log ft$ value close to those known for the given nuclei or for nuclei belonging to the neighboring region. Small deviations of the predicted and experimental GT resonance centroids suggest that the parameter χ should be fixed by fitting the centroids within the GRFR pn QRPA. By contrast with the standard pn QRPA models where the strength of the p-p interaction does not affect the position of the GT resonance centroids, here the attractive interaction contributes to the distribution of the β^- strength. Therefore, the two strengths should be fixed at the same time either by fitting two pieces of data, the GT resonance centroid and the $\log ft$ value of one decay of the intermediate odd-odd nucleus, or by fixing the $\log ft$ values corresponding to the single- β decays of the odd-odd intermediate nucleus.

Before closing let us enumerate the results of our numerical analysis.

- (i) Based on the matrix elements of the transition operator from the parent or daughter nucleus to the intermediate odd-odd nucleus, the β^- and β^+ strength distributions are plotted in Figs. 3–5. For ^{76}Ge , ^{82}Se , and $^{128,130}\text{Te}$ the results for the β^- strength have been compared with the corresponding experimental data. The centroids of the experimental peaks are fairly well reproduced.
- (ii) Note that, despite the fact that the results for the β^- transition strength distribution in $^{128,130}\text{Te}$ do not reproduce the corresponding experimental profile, the total strength is quite well described.
- (iii) Results for the summed strength $B(\text{GT}^-)$ agree quite well with the existing experimental data. Also the summed $B(\text{GT}^+)$ strengths for ^{76}Ti and ^{76}Se agree reasonably well with the corresponding experimental data.
- (iv) The calculated half-lives are in good agreement with the experimental data.
- (v) Results for the $\log ft$ values associated with the β^- and β^+ or EC transitions of the intermediate odd-odd nuclei are given in Table V.
- (vi) In general, the results for the double- β transition are consistent with those for single- β^- and $-\beta^+$ transitions of parent and daughter nuclei, respectively.

In conclusion, the present calculations prove that the GRFR pn QRPA is able to describe in a realistic manner $2\nu\beta\beta$ decay and moreover satisfies the ISR. The features that require some further improvements are also mentioned.

ACKNOWLEDGMENTS

This work was supported by the Romanian Ministry for Education Research Youth and Sport through CNCISIS projects and Grant No. ID-2/5.10.2011.

APPENDIX

The submatrices involved in the GRFR pn QRPA equations are given by the following expressions:

$$\begin{aligned}
 (A_{11})_{p_1n_1;pn} &= E^{\text{ren}}(pn)\delta_{pn;p_1n_1} + 2\chi\sigma_{p_1n_1;pn}^{(1)T}, \\
 (A_{12})_{p_1n_1;pn} &= 0, \quad (B_{11})_{p_1n_1;pn} = 0, \\
 (B_{12})_{p_1n_1;pn} &= 2\chi\sigma_{p_1n_1;pn}^{(1)T}, \\
 (A_{21})_{p_1n_1;pn} &= 0, \quad (B_{22})_{p_1n_1;pn} = 0, \\
 (A_{22})_{p_1n_1;pn} &= |E^{\text{ren}}(pn)|\delta_{pn;p_1n_1} + 2\chi\sigma_{p_1n_1;pn}^{(1)T}, \\
 (B_{21})_{p_1n_1;pn} &= 2\chi\sigma_{p_1n_1;pn}^{(1)T}.
 \end{aligned} \tag{A1}$$

-
- [1] H. Primakof and S. Rosen, *Rep. Prog. Phys.* **22**, 125 (1959).
 [2] W. C. Haxton and G. J. Stephenson Jr., *Prog. Part. Nucl. Phys.* **12**, 409 (1984).
 [3] J. D. Vergados, *Phys. Rep.* **361**, 1 (2001).
 [4] J. Suhonen and O. Civitarese, *Phys. Rep.* **300**, 123 (1998).
 [5] T. Tomoda, *Re. Prog. Phys.* **54**, 53 (1991).
 [6] A. Faessler, *Prog. Part. Nucl. Phys.* **21**, 183 (1988).
 [7] A. A. Raduta, *Prog. Part. Nucl. Phys.* **48**, 233 (2002).
 [8] A. A. Raduta, A. Faessler, and S. Stoica, *Nucl. Phys. A* **534**, 149 (1991).
 [9] A. A. Raduta, A. Faessler, S. Stoica, and W. Kaminsky, *Phys. Lett. B* **254**, 7 (1991).
 [10] J. Toivanen and J. Suhonen, *Phys. Rev. Lett.* **75**, 410 (1995).
 [11] A. A. Raduta, C. M. Raduta, W. Kaminski, and A. Faessler, *Nucl. Phys. A* **634**, 497 (1998).
 [12] A. A. Raduta, C. M. Raduta, and B. Codirla, *Nucl. Phys. A* **678**, 382 (2000).
 [13] A. A. Raduta, F. Simkovich, and A. Faessler, *J. Phys. G* **26**, 793 (2000).
 [14] C. M. Raduta and A. A. Raduta, *Nucl. Phys. A* **756**, 153 (2005).
 [15] C. M. Raduta and A. A. Raduta, *Phys. Rev. C* **82**, 068501 (2010).
 [16] C. M. Raduta and A. A. Raduta, *J. Phys. G* **38**, 055102 (2011).
 [17] A. A. Raduta, D. S. Delion, and N. Lo Iudice, *Nucl. Phys. A* **564**, 185 (1993).
 [18] A. A. Raduta, A. Escuderos, A. Faessler, E. Moya de Guerra, and P. Sarriguren, *Phys. Rev. C* **69**, 064321 (2004).
 [19] A. A. Raduta, C. M. Raduta, and A. Escuderos, *Phys. Rev. C* **71**, 024307 (2005).
 [20] S. G. Nilsson, *Mat. Fys. Medd. Dan. Vidensk. Selsk.* **29**, 16 (1955).
 [21] P. Ring and P. Shuck, *The Nuclear Many-Body Problem* (Springer, New York, 1980), p. 76.
 [22] Vadim Rodin and Amand Faessler, *Phys. Rev. C* **66**, 051303(R) (2002).
 [23] M. E. Rose, *Elementary Theory of Angular Momentum* (Wiley, New York, 1957).
 [24] N. Lo Iudice, A. A. Raduta, and D. S. Delion, *Phys. Rev. C* **50**, 127 (1994).
 [25] A. A. Raduta and R. Budaca, *Ann. Phys. (NY)*, DOI: 10.1016/j.aop.2011.10.004 (2011).
 [26] G. A. Lalazissis, S. Raman, and P. Ring, *At. Data Nucl. Data Tables* **71**, 1 (1999).
 [27] P. Möller, J. R. Nix, W. D. Myers, and W. J. Swiateski, *At. Data Nucl. Data Tables* **59**, 185 (1995).
 [28] H. Homma, E. Bender, M. Hirsch, K. Muto, H. V. Klapdor-Kleingrothaus, and T. Oda, *Phys. Rev. C* **54**, 2972 (1996).
 [29] B. D. Anderson *et al.*, *Phys. Rev. C* **31**, 1161 (1985).
 [30] R. Madey *et al.*, *Phys. Rev. C* **40**, 540 (1989).
 [31] L. Zamick and N. Auerbach, *Phys. Rev. C* **26**, 2185 (1982).
 [32] K. Grotz, H. V. Klapdor, and J. Metzinger, *J. Phys. G* **9**, 169 (1983).
 [33] J. Hirsch and F. Krmpotic, *Phys. Rev. C* **41**, 792 (1990).
 [34] J. Hirsch, E. Bauer, and F. Krmpotic, *Nucl. Phys. A* **516**, 304 (1990).
 [35] A. A. Raduta, O. Haug, F. Simkovic, and Amand Faessler, *Nucl. Phys. A* **671**, 255 (2000).
 [36] R. Helmer *et al.*, *Phys. Rev. C* **55**, 2802 (1997).
 [37] H. Dohmann *et al.*, *Phys. Rev. C* **78**, 041602(R) (2008).
 [38] K. Yako *et al.*, *Phys. Rev. Lett.* **103**, 012503 (2009).
 [39] W. P. Alford *et al.*, *Nucl. Phys. A* **514**, 49 (1990).
 [40] E.-W. Grewe *et al.*, *Phys. Rev. C* **76**, 054307 (2007).
 [41] E.-W. Grewe *et al.*, *Phys. Rev. C* **78**, 044301 (2008).
 [42] K. Grotz and H. V. Klapdor, *Phys. Lett. B* **157**, 242 (1985).
 [43] M. Hirsch *et al.*, *Phys. Rep.* **242**, 403 (1994).
 [44] X. R. Wu *et al.*, *Commun. Theor. Phys.* **20**, 453 (1993).
 [45] J. G. Hirsch, O. Castanos, P. O. Hess, and O. Civitarese, *Nucl. Phys. A* **589**, 445 (1995).
 [46] A. Balysh *et al.*, *Phys. Rev. Lett.* **77**, 5186 (1996).
 [47] A. S. Barabash, *Phys. Rev. C* **81**, 035501 (2010).
 [48] F. T. Avignone III *et al.*, *Phys. Lett. B* **256**, 559 (1991).
 [49] S. R. Elliott, A. A. Hahn, and M. K. Moe, *Phys. Rev. Lett.* **59**, 2020 (1987).
 [50] S. R. Elliott and P. Vogel, *Annu. Rev. Nucl. Part. Sci.* **52**, 115 (2002); A. S. Barabash, *Czech. J. Phys.* **52**, 567 (2002).
 [51] E. W. Hennecke, O. K. Manuel, and D. D. Sabu, *Phys. Rev. C* **11**, 1378 (1975).
 [52] A. A. Raduta, N. Lo Iudice, and I. I. Ursu, *Nucl. Phys. A* **584**, 84 (1995).
 [53] J. Lin *et al.*, *Nucl. Phys. A* **481**, 477 (1988).
 [54] A. L. Klimenko *et al.*, *Nucl. Instrum. Methods Phys. Res. B* **16**, 446 (1986).
 [55] C. Arpesella *et al.*, *Europhys. Lett.* **27**, 29 (1994).
 [56] Jean Blachot, *Nucl. Data Sheets* **92**, 455 (2001).
 [57] D. De Frenne and E. Jacobs, *Nucl. Data Sheets* **89**, 481 (2000).
 [58] C. M. Lederer and V. S. Shirley, *Table of Isotopes*, 7th ed. (Wiley, New York, 1978), p. 631.
 [59] M. Kanbe and K. Kitao, *Nucl. Data Sheets* **94**, 227 (2001).
 [60] L. Pacearescu, V. Rodin, F. Simkovic and Amand Faessler, *Phys. Rev. C* **68**, 064310 (2003).
 [61] O. Civitarese, M. Reboiro, and J. G. Hirsch, *Phys. Rev. C* **71**, 014318 (2005).
 [62] O. Civitarese *et al.*, *Nucl. Phys. A* **524**, 404 (1991).
 [63] R. V. Jolos and W. Rybarska-Nawrocka, *Z. Phys. A* **296**, 73 (1980).